

Electronic Supplementary Information

Simultaneous quantification of serum albumin and gamma globulin using Zn(II)-metallo-surfactant via coffee ring pattern

Aastha,^{† a} Priyanka^{† a} and Subhabrata Maiti^{* a}

† These authors contributed equally.

Department of Chemical Sciences, Indian Institute of Science Education and Research (IISER) Mohali,
Knowledge City, Manauli 140306, India

Table of Contents

1. Experimental Section	S2
2. Fluorescence Study.....	S4
3. Zeta Potential Measurements.....	S9
4. Circular Dichroism Study.....	S10
5. TEM images.....	S11
6. Fluorescent Microscopic Images.....	S13
7. Coffee Ring Patterns with C ₁₆ DPA•Zn ²⁺	S14
- Study of ring formation kinetics, AFM and SEM, contact angle, different pH, salt, and temperature	
8. DLS Measurements with Time.....	S32
9. Anisotropy Measurements.....	S33
10. Coffee Ring Pattern with FITC tagged Proteins.....	S34
11. Coffee Ring Patterns with CTAB.....	S35
12. Coffee Ring Patterns with SDS.....	S35
13. Coffee Ring Patterns with Serum.....	S36
14. References.....	S38

1. Experimental Section

1.1 Materials and method

All commercially available reagents were used as received without any further purification. The chemicals bovine serum albumin, Sodium Chloride, HEPES, CDCl_3 , Sodium dodecyl sulfate, cetyltrimethylammonium bromide, and Zinc Nitrate were procured from Sisco Research Laboratory

Human serum were purchased from Sigma-Aldrich. HPLC-grade methanol and acetonitrile purchased from Sigma-Aldrich were used.

The fluorescence microscopic images were captured using a Zeiss Axis Observer 7 microscope with an AxioCam 503 Mono 3 Megapixel with ZEN 2 software.

The Dynamic Light Scattering (DLS) data was recorded on Horiba Scientific Nanoparticle Analyzer SZ-100V2. In order to measure the size, and zeta potential, for the entire study 1 μM ALB, 1 μM GGB, 50 μM Zn(II)-metallo surfactant, 1 mM CTAB, 10 mM SDS were used.

UV-vis studies were performed using a Varian Cary 60 (Agilent Technologies) spectrophotometer. The total reaction volume in the cuvette was fixed at 1 ml, and a cuvette with a path length of 1 cm was used for the entire kinetic study. All measurements were performed at 25 °C.

Gamma-globulin was dissolved in 0.9% NaCl solution. The molecular weight for gamma-globulin is 155-160 kDa and extinction coefficient $E^{1\%} = 13.8$. Using this data, the molar extinction coefficient calculated was around $\epsilon = 210,000 \text{ M}^{-1}\text{cm}^{-1}$ which was used further throughout the studies^{[S1], [S2]}.

Fluorescence measurements were performed using Cary Eclipse Fluorescence Spectro-fluorometer.

Circular Dichroism (CD) Measurements were performed using Chirascan Spectrophotometer (Applied Photophysics) using a 1 mm path length quartz cell. The spectra were recorded over a scan range of 200-280 nm. For each sample three repeated measurements were recorded.

Innova atomic force microscope (Bruker) operating in tapping mode was used for AFM experiment. Imaging was performed using a silicon Tip on a cantilever (Bruker) and images were analyzed using Gwyddion software. For Atomic Force Microscopy (AFM), samples were prepared with 50 μM concentration of $\text{C}_{16}\text{DPA}\cdot\text{Zn}^{2+}$ and 1 μM ALB and 1 μM GGB in pH-7 5mM HEPES. 1.5 μL of the samples were deposited on a cleaned glass surface after incubation for 15- 20 min.

Time-correlated single-photon counting (TCSPC) was measured in (Horiba Jobin Yvon, NJ). The samples were excited using 440-nm NanoLED picosecond laser diodes.

The contact angle was measured by a drop shape analyzer-DSA25-KRUSS GmbH.

Steady-state anisotropy measurements were performed on an LS 55 luminescence spectrometer from Perkin Elmer at an excitation wavelength of 430 nm with a bandpass of 2.5 nm for excitation and 2.5 nm for emission.

The surfactant $\text{C}_{16}\text{DPA}\cdot\text{Zn}^{2+}$ was synthesized and characterized as reported in the literature^[S3].

1.2 Sample Preparation and Drop Deposition

For sample preparation, the proper amounts of buffer, surfactant solution, proteins and Coumarin153 were added in this order in an Eppendorf tube and left incubated for 20 minutes. Before each experiment, the suspensions were mixed for about 15 s. A drop (1.5 μL) was then immediately deposited on glass coverslip using a micropipette and was covered with a box to avoid air currents. All drying experiments were performed at 25 ± 1 °C. After drying the droplets, images of the coffee ring were captured using fluorescence microscopy. Similarly, using 0.1% blood serum, coffee ring formation was captured.

1.3 Imaging of the Deposits

Fluorescent Microscopic images of the deposited patterns were captured with an inverted optical microscope (Zeiss Axis Observer 7) equipped with an AxioCam 503 Mono 3 Megapixel. All images were acquired in similar illumination conditions and acquisition settings. They are displayed without any post-processing.

1.4 Measurement of Surface Potential (ζ) of conjugates

Mixtures held in Eppendorf tubes were shortly mixed (15 s), before being loaded in Zeta cuvette using a Micropipette. The surface potential of conjugates was measured utilizing a Horiba Scientific Nanoparticle Analyzer SZ-100V2. All experiments were performed at 25 °C. Each measurement lasted 60 s and was repeated ten times.

1.5 Tryptophan fluorescence studies with protein surfactant conjugates

Tryptophan fluorescence studies was performed with 1 μM of proteins namely ALB and GGB with titration of surfactants ($\text{C}_{16}\text{DPA}\cdot\text{Zn}^{2+}$, CTAB, SDS) in a quartz cuvette of 1 cm pathlength. The excitation wavelength was 280 nm and emission spectra were recorded in between 300 – 500 nm. Further binding constant were calculated using a double logarithmic plot [$\log(F_0-F/F)$] vs \log [surfactant]. The excitation and emission slit width were 5 and 5 nm respectively.

1.6 Measurement of anisotropy

The steady state anisotropy measurements of Zn(II)-metallo surfactant with proteins (ALB and GGB) in presence of C153 were performed on an LS 55 luminescence spectrometer from Perkin Elmer. For steady state anisotropy samples were made in eppendorf tube and left incubated for 20 minutes. Before experiment, the suspensions were mixed for about 15 s and poured in quartz cuvette of 1cm pathlength for recording the spectra. The excitation wavelength was 430 nm and emission spectra were recorded in between 450 nm – 700 nm with excitation and emission bandpass 2 and 2.5 nm respectively. In case of surfactant and surfactant-protein conjugate the wavelength maxima was around 520 nm while in control experiments the maxima was 550 nm. The final concentration of surfactant, ALB, GGB and C153 was 50 μM , 1 μM , 1 μM and 2 μM respectively during the experiment.

1.8 Transmission Electron Microscopy (TEM) Imaging

To visualize aggregates in the protein-surfactant conjugate system, a JEOL JEM-F200 microscope was used. For preparing TEM samples, 50 μM Zn(II)-metallo surfactant was used in the presence of ALB (1 μM), GGB (1 μM). After 20 minutes of incubation, around 5–7 μL of sample was cast on a carbon-coated 300-mesh copper grid and dried in air. Then, 4 μL of a 0.1% uranyl acetate solution was added to the grid for staining and allowed to soak for 10 s, it was dried by placing a piece of Whatman filter paper on the side of the grid. The sample was then dried under vacuum before imaging.

1.9 Preparation of FITC Tagged ALB and GGB

FITC-tagged ALB was prepared as given in literature.^[54] 1 mg/ml FITC was dissolved in DMSO, then 100 μ l of this was mixed with 5 mg/ml of ALB. The solution was kept under the dark at 4 °C for 5 to 6 hrs. After that, the ongoing reaction of tagging was quenched by the addition of 50 mM of ammonium chloride and the mixture was kept for more 2 hrs. Then the reaction mixture was passed through a column made up of Sephadex G-25 and the formed conjugate was purified through the column with 5 mM HEPES buffer (pH= 7). The eluted samples were collected in the different vials and their UV absorption spectra were recorded in which FITC-BSA conjugate showed absorption maxima at 280nm peak and FITC at 495nm. Tagging efficiency of BSA was found 0.5, means a single enzyme has an average of 0.5 FITC molecule. Similarly, FITC-tagged GGB was prepared, and for the purification 0.9% NaCl solution was passed through the Sephadex G-25 column. Tagging efficiency of GGB was found 0.9, means a single enzyme has an average of 0.9 FITC molecule.

1.10 Image J measurements

Using ImageJ software, after calibrating the images, the intensity profile data with respect to distance was collected. Using the data, the area under the curve was calculated to measure the fluorescence intensity.

1.10 Scanning Electron Microscopy (SEM) Imaging

For preparing SEM samples, 50 μ M Zn(II)-metallo-surfactant was used in the presence of ALB (1 μ M), and GGB (1 μ M). After 20 minutes of incubation, around 1.5 μ L of the sample was cast on silicon wafers and dried overnight. Prior to the examination, air-dried samples were coated with gold using a JEOL JEC-3000FC sputter coater (Leica Microsystems). Following this, the samples were imaged under an electron microscope.

2. Fluorescence Study:

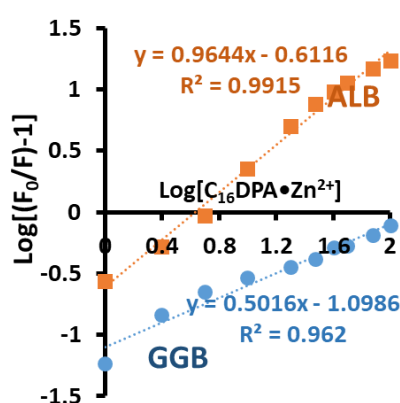


Fig. S1: (a) The plot of $\log[(F_0-F)/F]$ versus $\log [C_{16}DPA \bullet Zn^{2+}]$ for protein-surfactant conjugates ALB and GGB solutions (1 μ M) in the presence of $C_{16}DPA \bullet Zn^{2+}$ with the following concentrations: 0, 1, 5, 10, 25, 50 and 100 μ M. Experimental conditions: [HEPES] = 5 mM, pH 7.0, T = 25 °C.

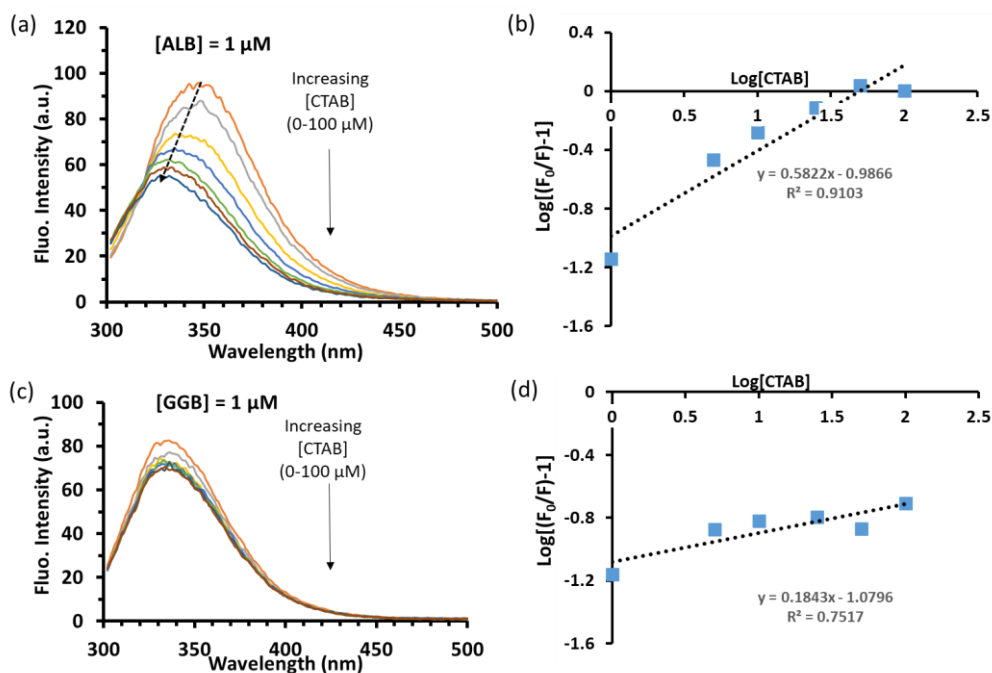


Fig. S2: Fluorescence emission spectra of (a) ALB and (c) GGB solutions (1 μM) in the presence of SDS with the following concentrations: 0 μM, 1 μM 10 μM, 20 μM, 50 μM and 100 μM; (b) & (d) the plot of $\log[(F_0 - F)/F]$ versus $\log [\text{CTAB}]$ for protein-surfactant conjugates. Experimental conditions: [HEPES] = 5 mM, pH 7.0, T = 25 °C.

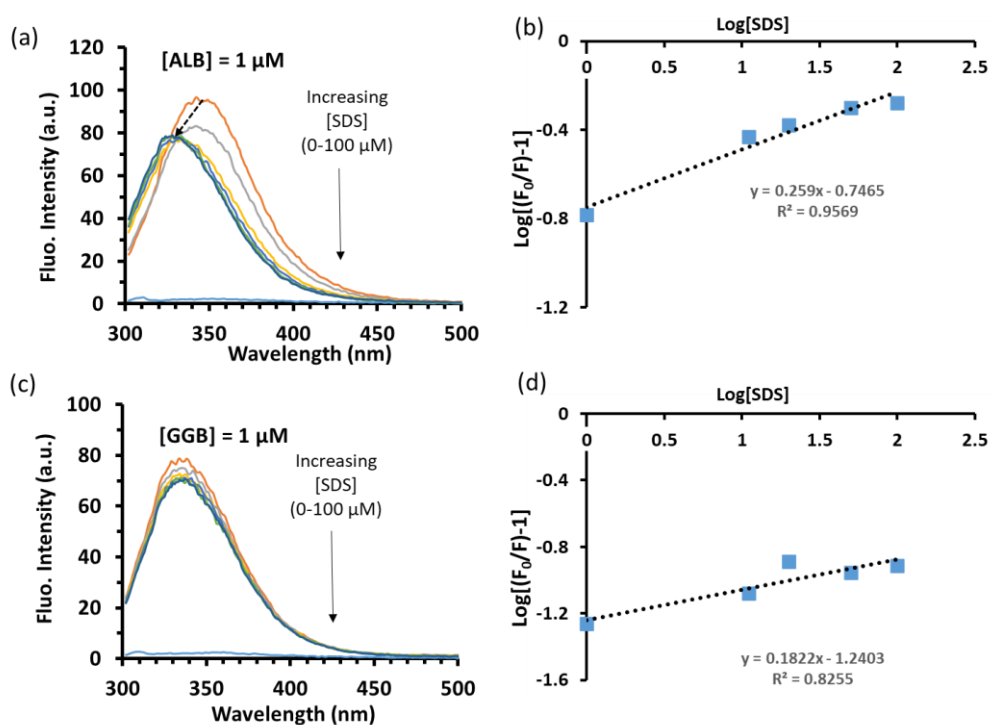


Fig. S3: Fluorescence emission spectra of (a) ALB and (b) GGB solutions (1 μM) in the presence of SDS with the following concentrations: 0 μM, 1 μM 10 μM, 20 μM, 50 μM and 100 μM; (b) & (d) the plot of $\log[(F_0 - F)/F]$ versus $\log [\text{SDS}]$ for protein-surfactant conjugates. Experimental conditions: [HEPES] = 5 mM, pH 7.0, T = 25 °C.

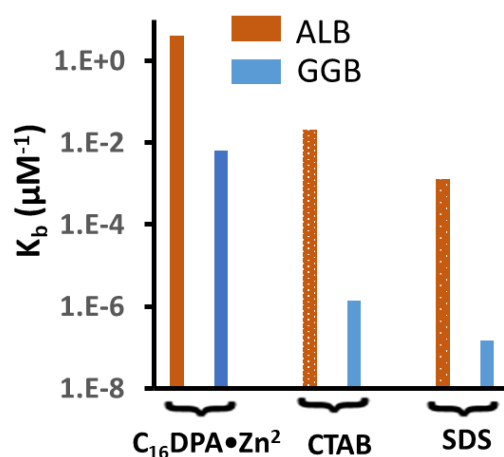


Fig. S4: Binding constant values between different surfactant ($\text{C}_{16}\text{DPA}\cdot\text{Zn}^{2+}$, CTAB, SDS) and ALB or GGB conjugate determined from fluorimetric surfactant titration curve as shown in Fig.S5(a). Experimental conditions: [HEPES] = 5 mM, pH 7.0, T = 25 °C.

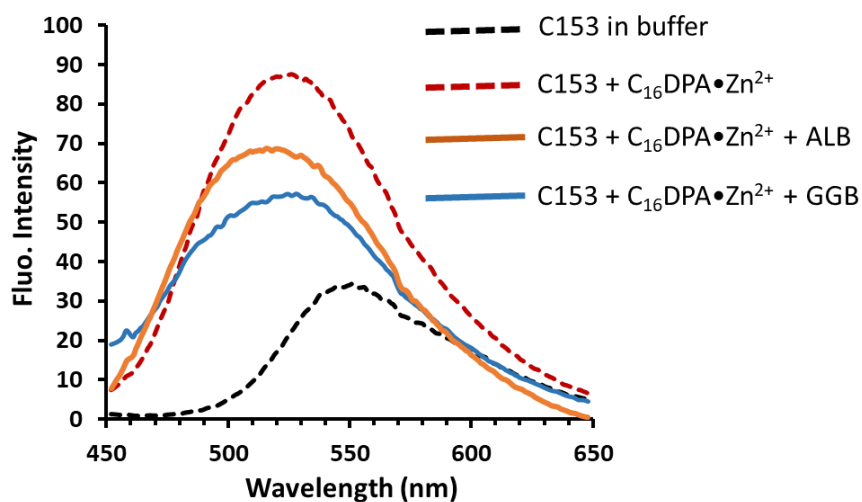


Fig. S5: Fluorescence emission spectra of ALB and GGB solutions in the presence of $\text{C}_{16}\text{DPA}\cdot\text{Zn}^{2+}$ using C153 as a hydrophobic probe. The blue shift of peaks in presence of surfactant and surfactant-protein conjugate verifies the hydrophobic residence propensity of C153. Experimental conditions: [ALB] & [GGB] = 1 μM [$\text{C}_{16}\text{DPA}\cdot\text{Zn}^{2+}$] = 50 μM , [C153] = 2 μM , Slit Width ex/em = 5/5 nm, [HEPES] = 5 mM, pH 7.0, T = 25 °C.

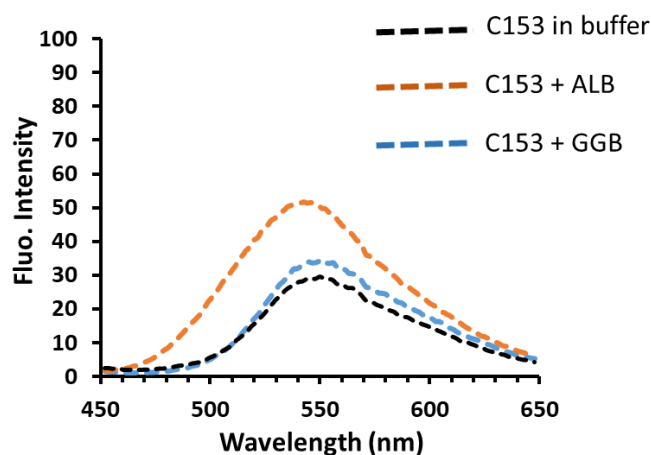


Fig. S6: Fluorescence emission spectra of ALB and GGB solutions using C153 as a hydrophobic probe. No blue Shift in peaks was observed in the case of only proteins. Experimental conditions: [ALB] & [GGB] = 1 μ M, [C153] = 2 μ M, Slit Width ex/em = 5/5 nm, [HEPES] = 5 mM, pH 7.0, T = 25 $^{\circ}$ C.

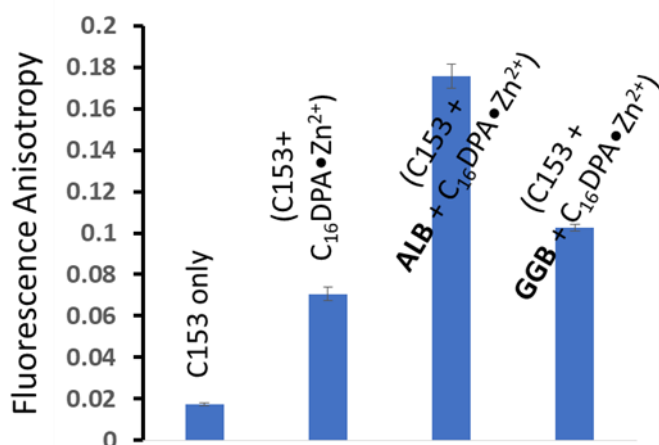


Fig. S7: Fluorescence anisotropy value of C153 (2.5 μ M) in absence and presence of C₁₆DPA•Zn²⁺ (50 μ M) and ALB or GGB (1 μ M). (Experimental conditions: [HEPES] = 5 mM, pH 7.0, T = 25 $^{\circ}$ C.

Fluorescence Lifetime measurement

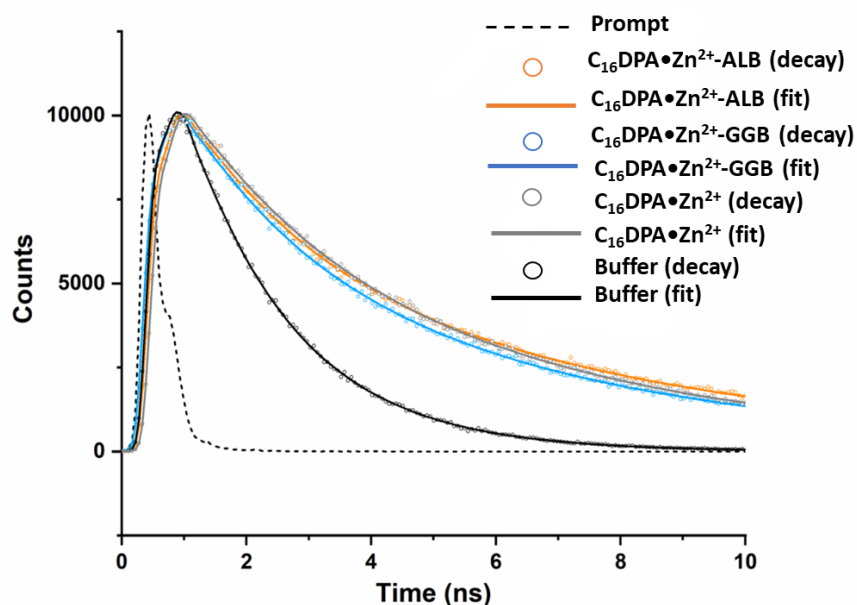


Fig. S8. Time-domain intensity decay of C153 in aqueous buffer, $[C_{16}DPA \cdot Zn^{2+}] = 50 \mu M$ and in presence and absence of ALB and GGB ($1 \mu M$), excited by a 440 nm laser (HEPES, 5 mM, pH 7).

Table S1. Lifetime, τ , (ns) of C153 with $C_{16}DPA \cdot Zn^{2+}$ in absence and presence of ALB and GGB.

	τ_1 (ns)	τ_2 (ns)	τ_3 (ns)	α_1	α_2	α_3	τ_{avg} (ns)	χ^2
1 μM C153	0.0925	1.68	---	4.83	95.17	---	1.6033 ± 0.02	1.28
50 μM $C_{16}DPAZn^{2+}$ +1μM C153	2.183	5.84	0.114	20.39	77.58	2.03	4.9780 ± 0.06	1.124
50 μM $C_{16}DPAZn^{2+}$ +1 μM GGB+1 μM C153	1.9	5.81	0.091	19.93	77.78	2.29	4.8997 ± 0.04	1.064
50 μM $C_{16}DPAZn^{2+}$ +1 μM ALB+1 μM C153	1.864	6.54	0.1018	17.22	80.83	1.95	5.6092 ± 0.05	1.144

Lifetime data also suggest residence of C153 probe in case of ALB-surfactant was in a more hydrophobic domain with more compact structure as lifetime value increased by almost 0.7 ns. In contrary for GGB, a slight decrease in lifetime value was observed compared to only surfactant, suggesting formation of less compact structure.

3. Zeta Potential Measurements:

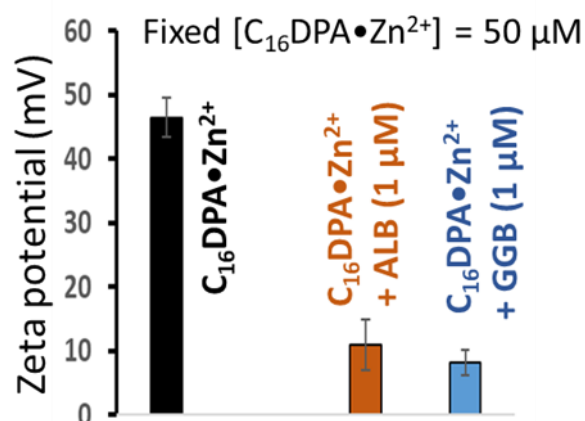


Fig. S9. Zeta potential values of $C_{16}DPA \bullet Zn^{2+}$ ($50 \mu M$) in absence and presence of ALB or GGB. Experimental conditions: $[HEPES] = 5 \text{ mM}$, $pH 7.0$, $T = 25 \text{ }^\circ\text{C}$.

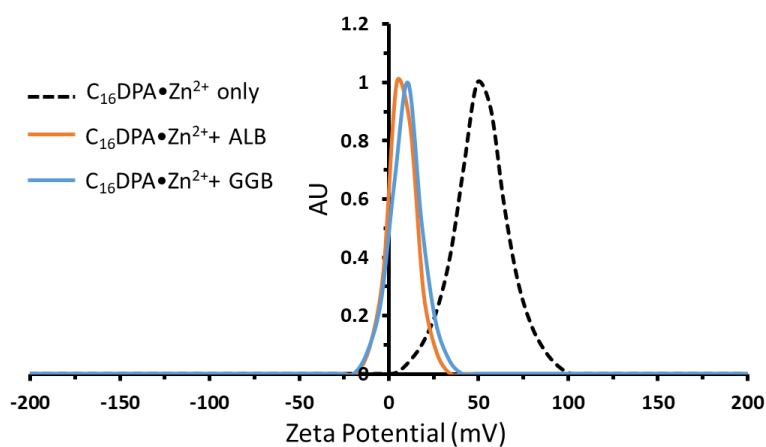


Fig. S10: Representative plots of Proteins (ALB and GGB) with Zn(II)-metallo-surfactant showing zeta potential values of each system. Experimental condition: $[ALB]: 1 \mu M$, $[GGB]: 1 \mu M$, $[C_{16}DPA \bullet Zn^{2+}]: 50 \mu M$, HEPES Buffer (5 mM , $pH = 7$), $T=25 \text{ }^\circ\text{C}$.

4. Circular Dichroism Study:

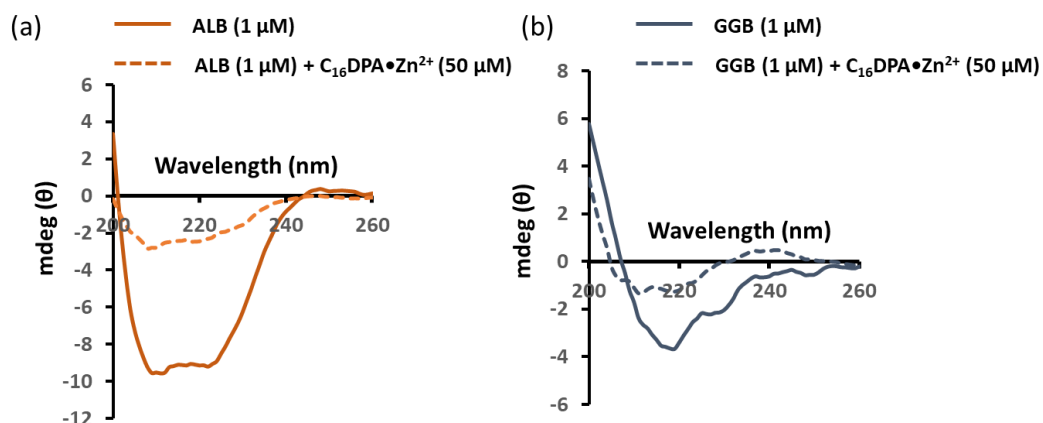


Fig. S11. Circular Dichroism (CD) spectra of (a) only ALB (1 μM) along with Zn(II)-metallo-surfactant (b) only GGB (1 μM) along with Zn(II)-metallo-surfactant in Buffer (HEPES, pH = 7). Experimental condition: [ALB] = 1 μM , [GGB] = 1 μM , [$\text{C}_{16}\text{DPA}\cdot\text{Zn}^{2+}$] = 50 μM , CD cuvette pathlength = 1 mm, HEPES buffer (5 mM, pH = 7), T = 25 $^{\circ}\text{C}$.

5. TEM images:

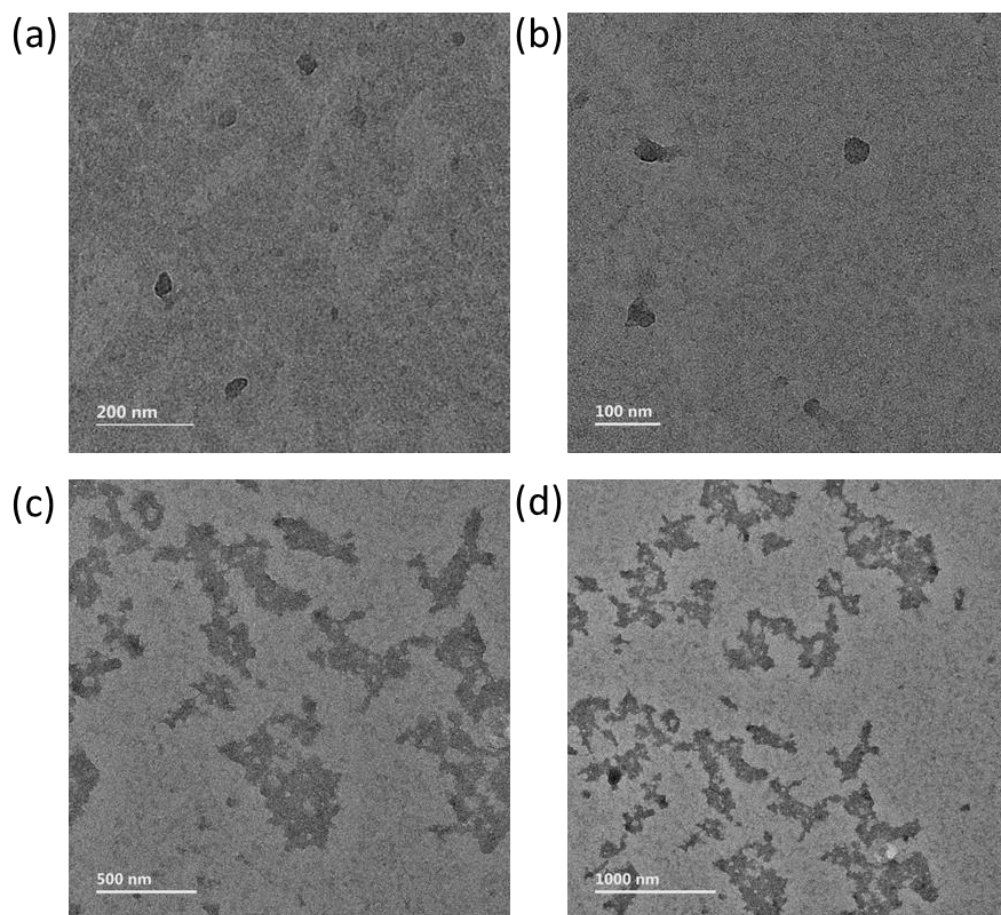
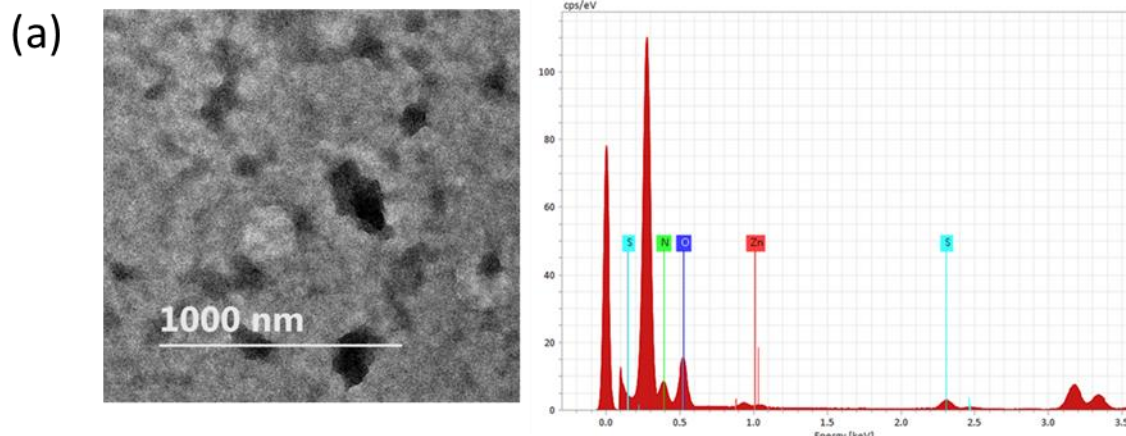
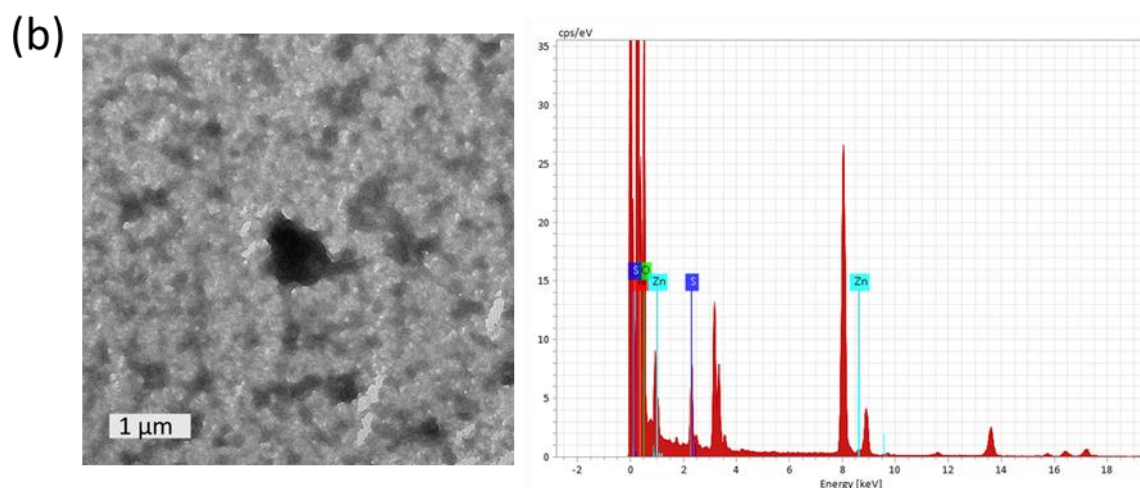


Fig. S12. TEM images of (a-b) ALB and (c-d) GGB with Zn(II)-metallo surfactant. 0.1% uranyl acetate solution was used to stain the grid. Experimental conditions: [ALB] & [GGB] = 1 μ M, [C₁₆DPA•Zn²⁺] = 50 μ M, [HEPES] = 5 mM, pH 7.0, T = 25 °C.



Acquisition.txt

Element	At. No.	Netto	Mass [%]	Mass Norm. [%]	Atom [%]	abs. error [%] (3 sigma)
Zinc	30	2999	5.28	5.28	1.39	0.79
Nitrogen	7	19632	25.99	25.99	31.96	2.52
Oxygen	8	49154	55.10	55.10	59.32	5.09
Sulfur	16	13745	13.64	13.64	7.33	1.45
		Sum	100.00	100.00	100.00	



Acquisition

Element	At. No.	Netto	Mass [%]	Mass Norm. [%]	Atom [%]	abs. error [%] (3 sigma)
Nitrogen	7	29792	30.28	30.28	36.05	2.85
Oxygen	8	63450	54.61	54.61	56.92	5.01
Sulfur	16	15758	12.01	12.01	6.24	1.28
Zinc	30	2297	3.11	3.11	0.79	0.51
		Sum	100.00	100.00	100.00	

Fig. S13. Transmission electron microscopy with energy-dispersive X-ray spectroscopy (TEM-EDX) analysis of (a) $C_{16}DPA \bullet Zn^{2+}$ -ALB and (b) $C_{16}DPA \bullet Zn^{2+}$ -GGB complex. Presence of Zn^{2+} confirms the presence of metallo-surfactant and sulphur (S) confirms the presence of protein in the complex.

6. Fluorescent Microscopic Images:

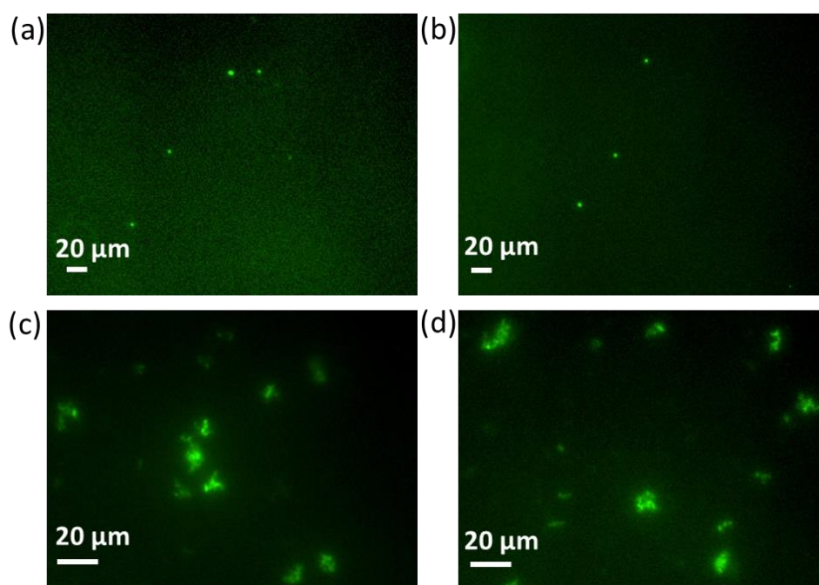
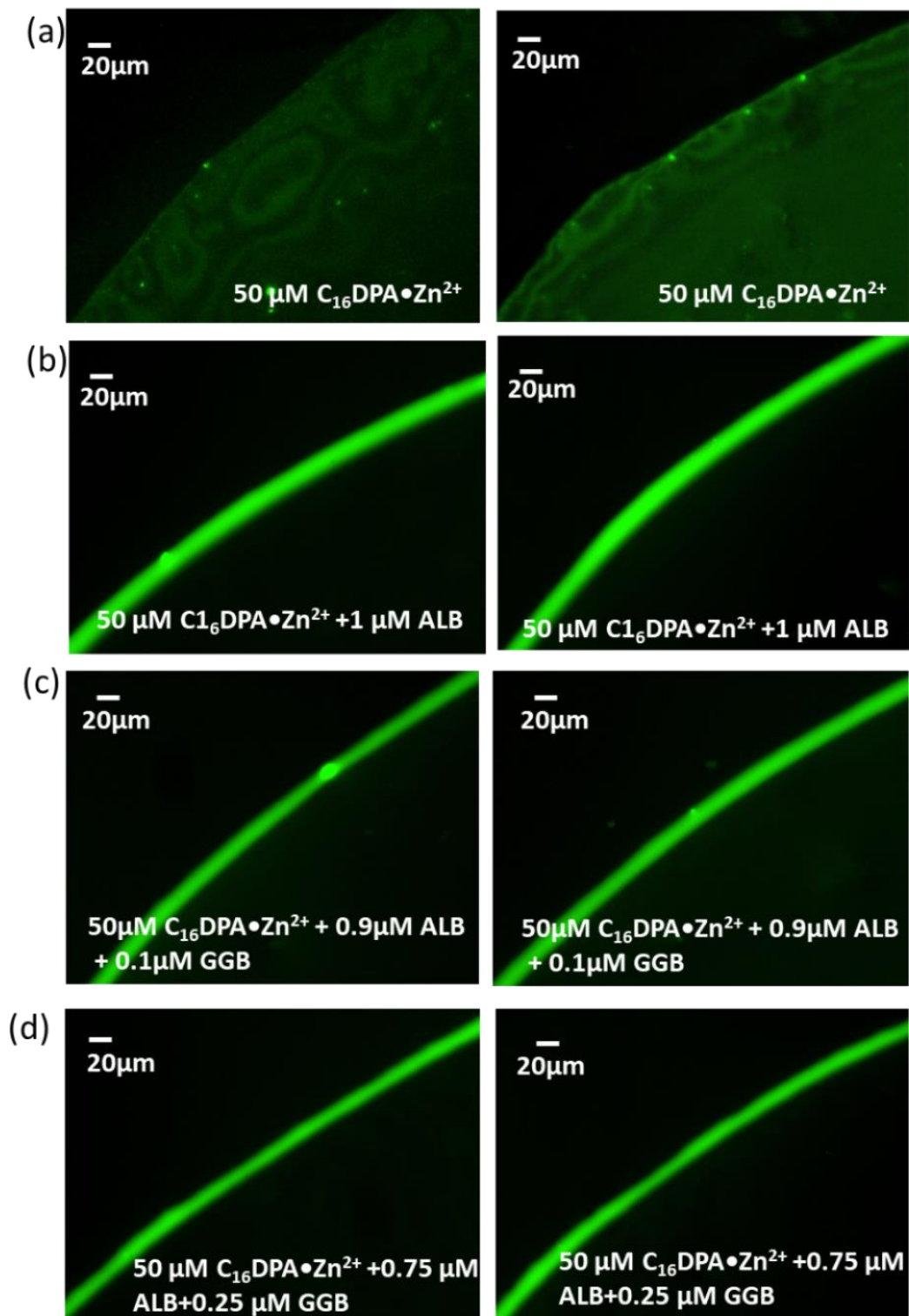


Fig. S14. Fluorescence microscopic images of (a-b) ALB and (c-d) GGB with Zn(II)-metallo surfactant. Images were captured after incubating the samples for 20 minutes. Experimental conditions: [ALB] & [GGB] = 1 μM , [C153] = 2 μM , [C₁₆DPA•Zn²⁺] = 50 μM , [HEPES] = 5 mM, pH 7.0, T = 25 °C.

7. Coffee Ring Patterns with $C_{16}DPA \bullet Zn^{2+}$:

7.1. Fluorescence Study



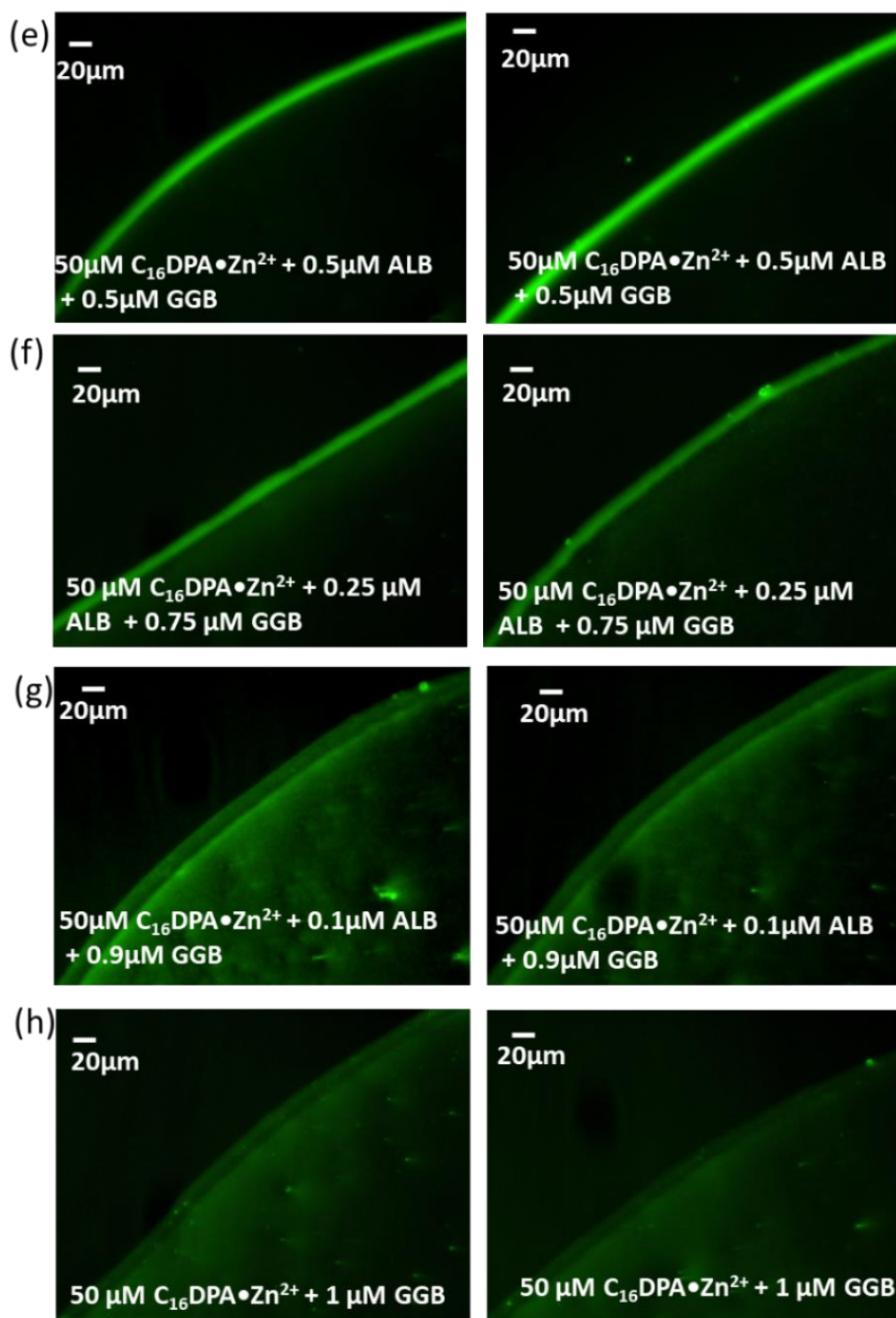


Fig. S15. Fluorescence microscopic images (a)-(h) of the spatiotemporal pattern of the ring-like structure formation after the evaporation of a droplet consisting of $C_{16}\text{DPA} \cdot \text{Zn}^{2+}$, mixed with probe C153 (2 μM) and different amount of ALB and GGB in buffer. Experimental conditions: Total $[\text{ALB}] + [\text{GGB}] = 1 \mu\text{M}$, $[\text{C153}] = 2 \mu\text{M}$, $[\text{C}_{16}\text{DPA} \cdot \text{Zn}^{2+}] = 50 \mu\text{M}$, $[\text{HEPES}] = 5 \text{ mM}$, $\text{pH } 7.0$, $T = 25 \text{ }^\circ\text{C}$.

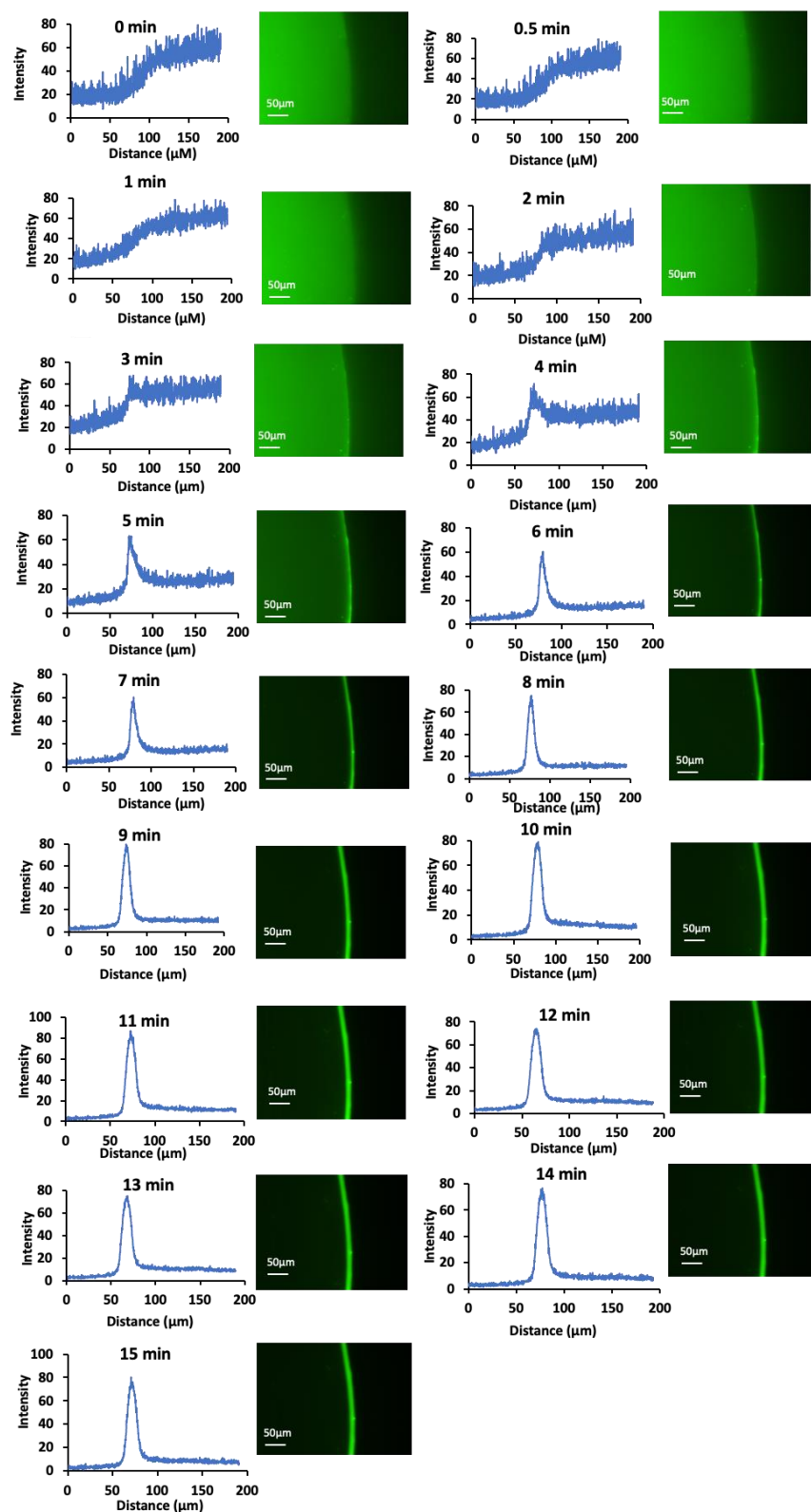


Fig. S16. Time evolution images of the ring growth for $C_{16}DPA \bullet Zn^{2+}$ -ALB complex. $[C_{16}DPA \bullet Zn^{2+}] = 50 \mu M$, $[ALB] = 1 \mu M$, $[C153] = 2 \mu M$. It suggests the ring formation started after 4 min of droplet addition.

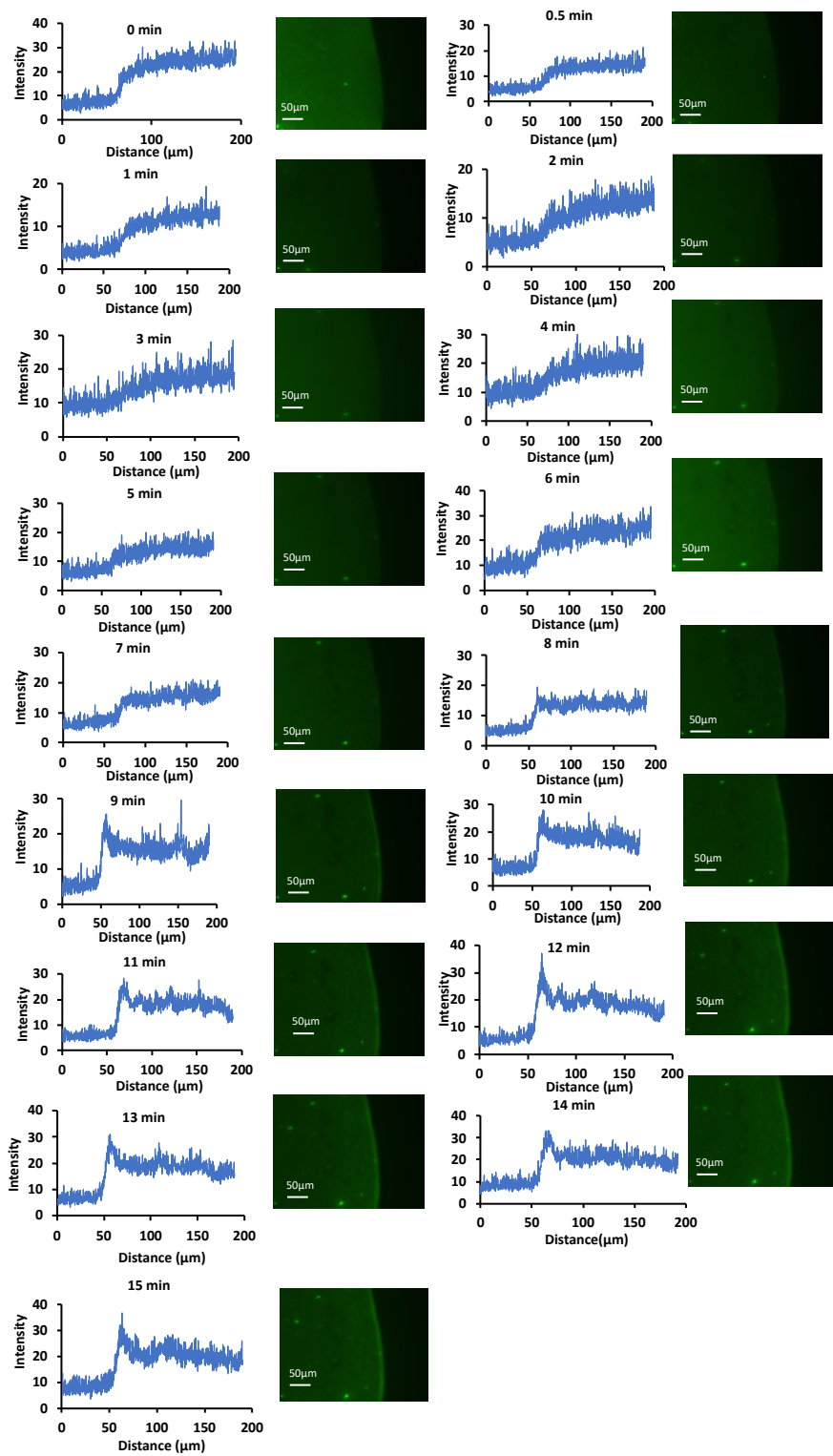


Fig. S17. Time evolution images of the ring growth for $C_{16}DPA \bullet Zn^{2+}$ -GGB complex. $[C_{16}DPA \bullet Zn^{2+}] = 50 \mu M$, $[GGB] = 1 \mu M$, $[C153] = 2 \mu M$. It suggests no prominent ring formation started even after 15 min of droplet addition.

7.2. AFM study:

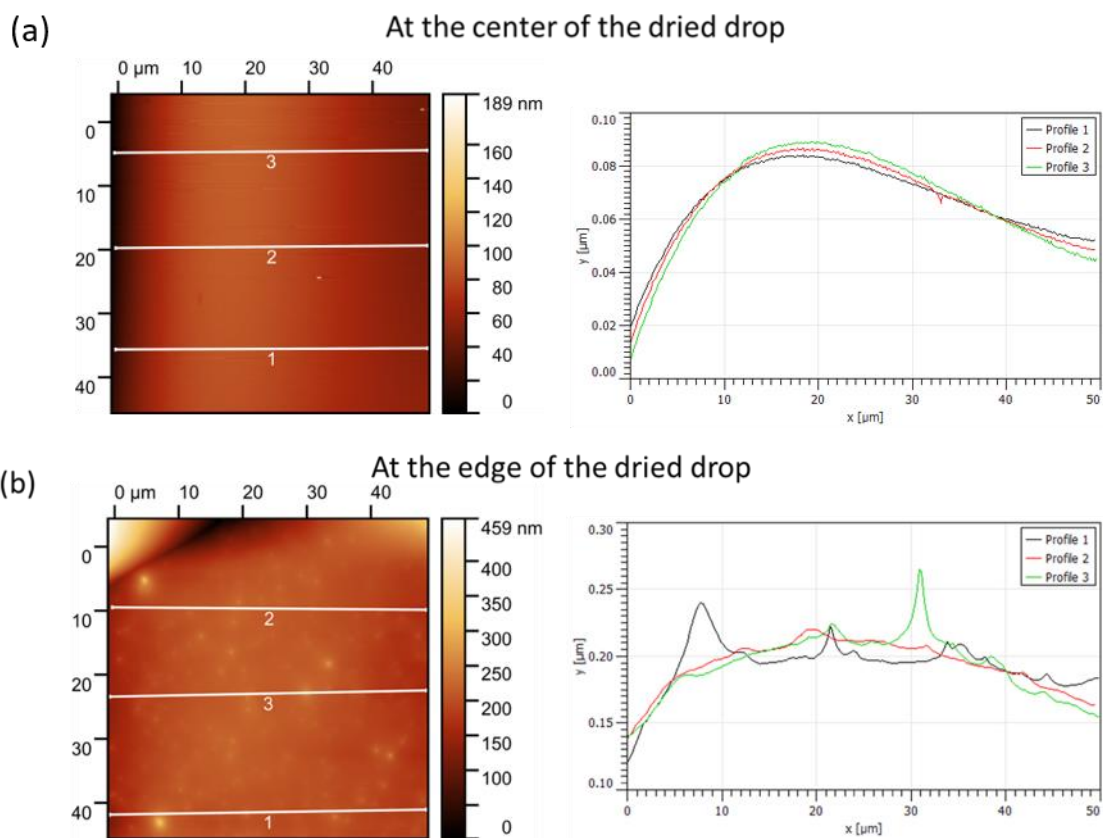


Fig. S18. AFM image and height profile diagram of $C_{16}DPA \bullet Zn^{2+}-ALB$ (a) at the center region and (b) at the edge of the dried drop casted on glass cover slip. $[C_{16}DPA \bullet Zn^{2+}] = 50 \mu M$, $[ALB] = 1 \mu M$.

From the height profile study, the height at the edge of the droplet was 150-250 nm, whereas in the center it is mostly 50-70 nm, upon scanning an area of $50 \times 50 \mu m^2$, suggesting formation of ring for $C_{16}DPA \bullet Zn^{2+}-ALB$ complex.

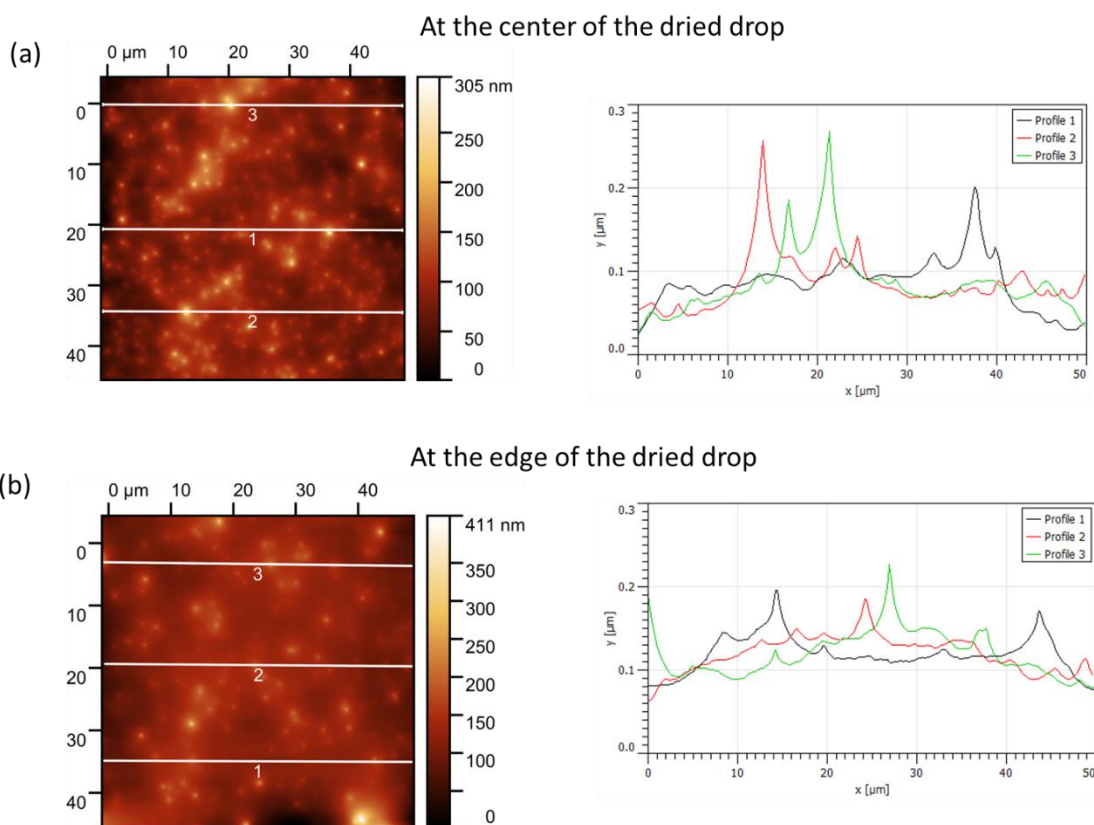


Fig. S19. AFM image and height profile diagram of $C_{16}DPA \bullet Zn^{2+}$ -GGB (a) at the center region and (b) at the edge of the dried drop casted on glass cover slip. $[C_{16}DPA \bullet Zn^{2+}] = 50 \mu M$, $[GGB] = 1 \mu M$.

From the height profile study, the height at the edge of the droplet was 100-150 nm and in the center, it is also around 100 nm, upon scanning an area of $50 \times 50 \mu m^2$, suggesting similar structural height pattern throughout the drop and no distinct formation of ring at the edge, even after evaporation for $C_{16}DPA \bullet Zn^{2+}$ -GGB complex.

7.3. SEM study:

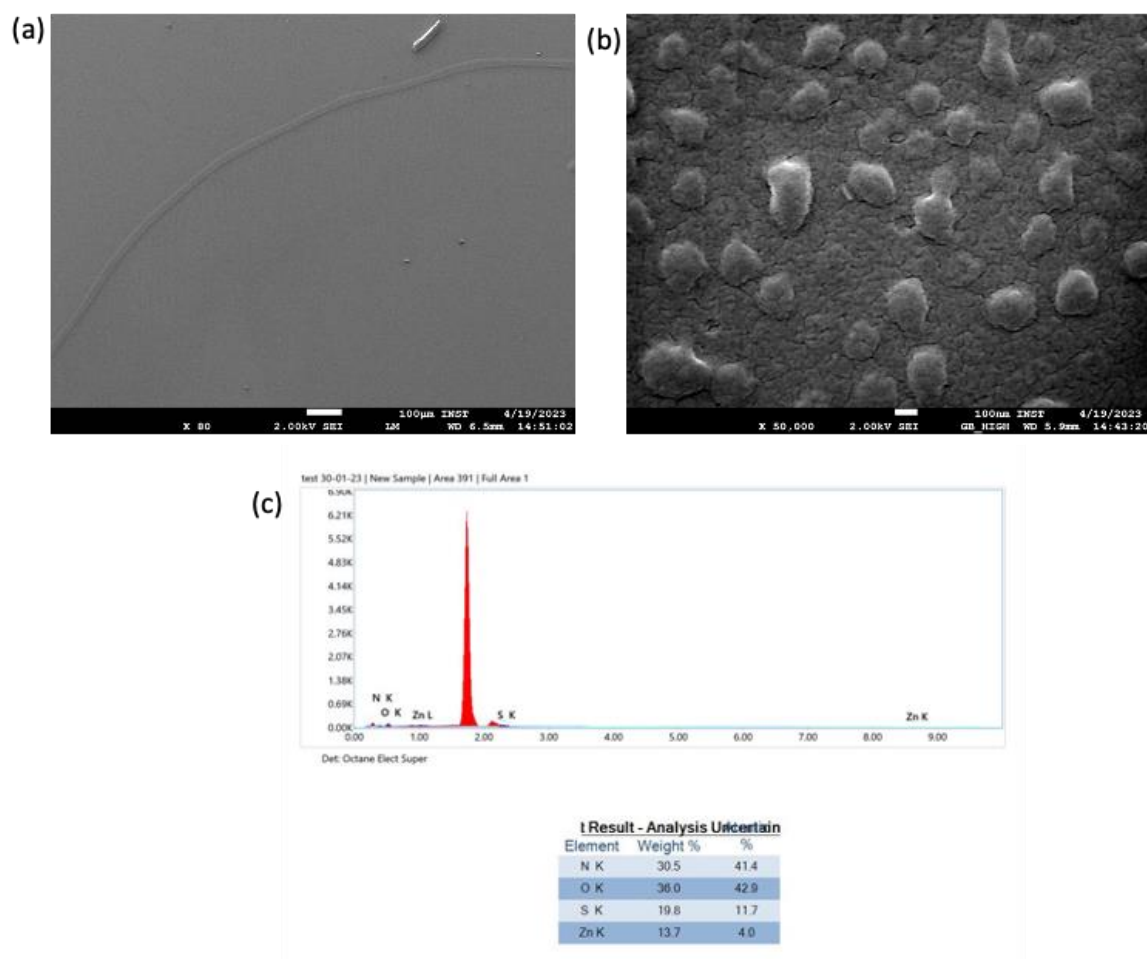
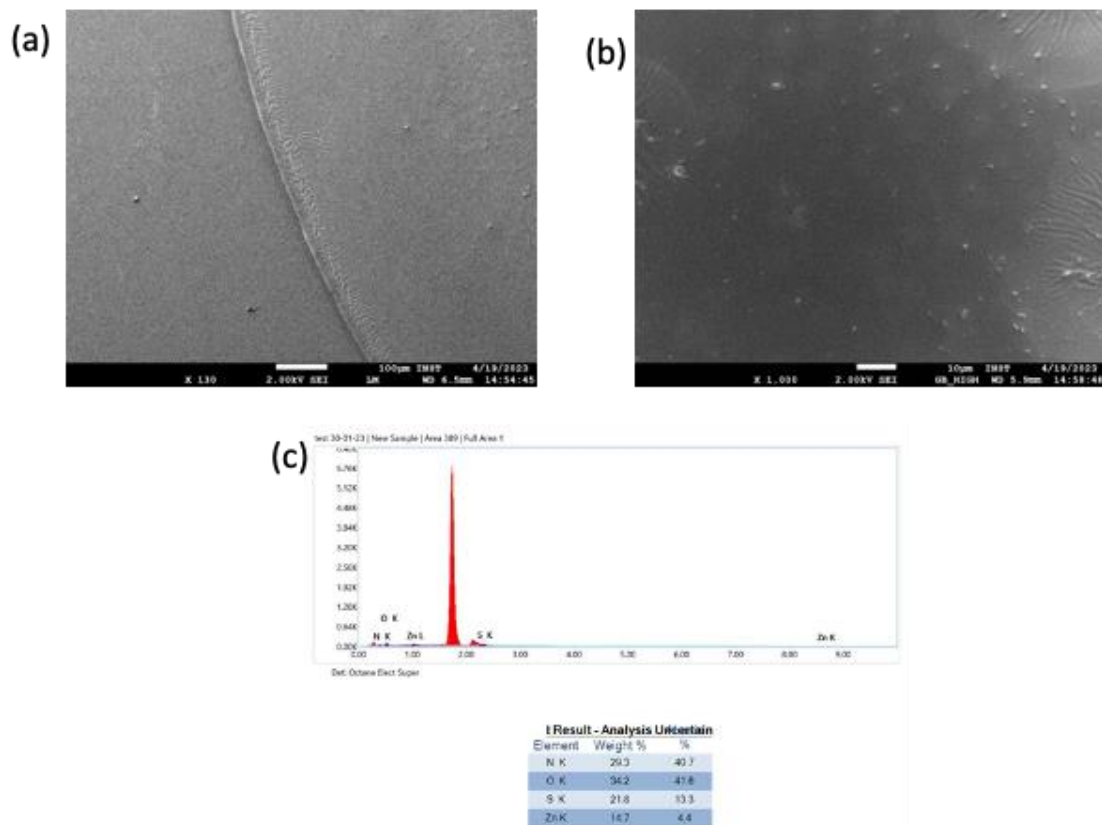


Fig. S20. (a) SEM images of the $C_{16}DPA \bullet Zn^{2+}$ -ALB complex showing the formation of coffee ring at the periphery of the droplet. (scale bar = 100 μm). (b) Zoomed images of the ring, showing accumulation of conjugate (scale bar = 100 nm). (c) Scanning electron microscopy with energy-dispersive X-ray spectroscopy (SEM-EDX) analysis showed presence of Zn^{2+} which confirms the presence of metallo-surfactant and sulphur (S) confirms the presence of protein in the complex.



7.4. Coffee ring formation at different contact angle

In glass surface

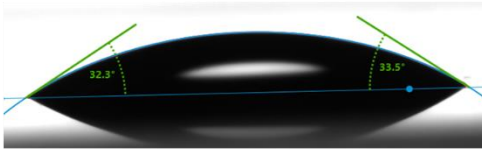
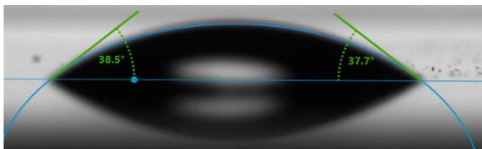
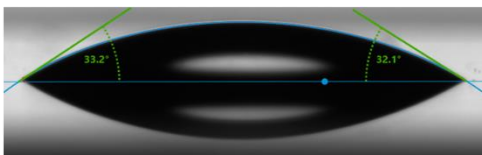
<u>System</u>	<u>Contact angle</u>	<u>Representative images</u>
Only C ₁₆ DPA•Zn ²⁺	33 ± 0.5°	
C ₁₆ DPA•Zn ²⁺ + ALB	36 ± 2.5°	
C ₁₆ DPA•Zn ²⁺ + GGB	32.5 ± 0.7°	

Fig. S22. Contact angle values and representative images of only C₁₆DPA•Zn²⁺, C₁₆DPA•Zn²⁺-ALB and C₁₆DPA•Zn²⁺-GGB complex on glass surface.

In Plastic (Polystyrene)

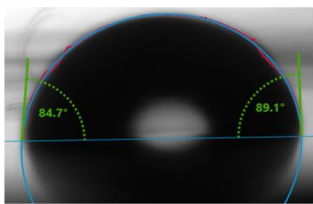
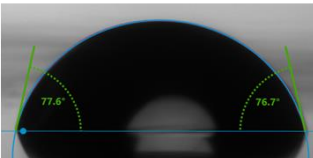
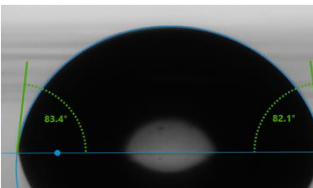
<u>System</u>	<u>Contact angle</u>	<u>Representative images</u>
Only C ₁₆ DPA•Zn ²⁺	86 ± 3°	
C ₁₆ DPA•Zn ²⁺ + ALB	78 ± 2.5°	
C ₁₆ DPA•Zn ²⁺ + GGB	82 ± 4°	

Fig. S23. Contact angle values and representative images of only C₁₆DPA•Zn²⁺, C₁₆DPA•Zn²⁺-ALB and C₁₆DPA•Zn²⁺-GGB complex on plastic (polystyrene) surface.

In RainX coated glass slide

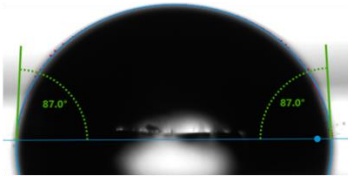
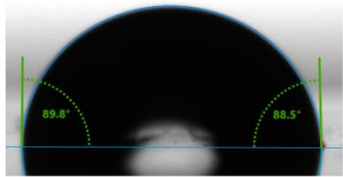
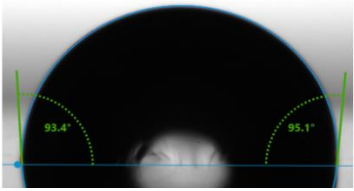
<u>System</u>	<u>Contact angle</u>	<u>Representative images</u>
Only C ₁₆ DPA•Zn ²⁺	87 ± 2°	
C ₁₆ DPA•Zn ²⁺ + ALB	88 ± 1°	
C ₁₆ DPA•Zn ²⁺ + GGB	93 ± 2°	

Fig. S24. Contact angle values and representative images of only C₁₆DPA•Zn²⁺, C₁₆DPA•Zn²⁺-ALB and C₁₆DPA•Zn²⁺-GGB complex on RainX-coated glass surface.

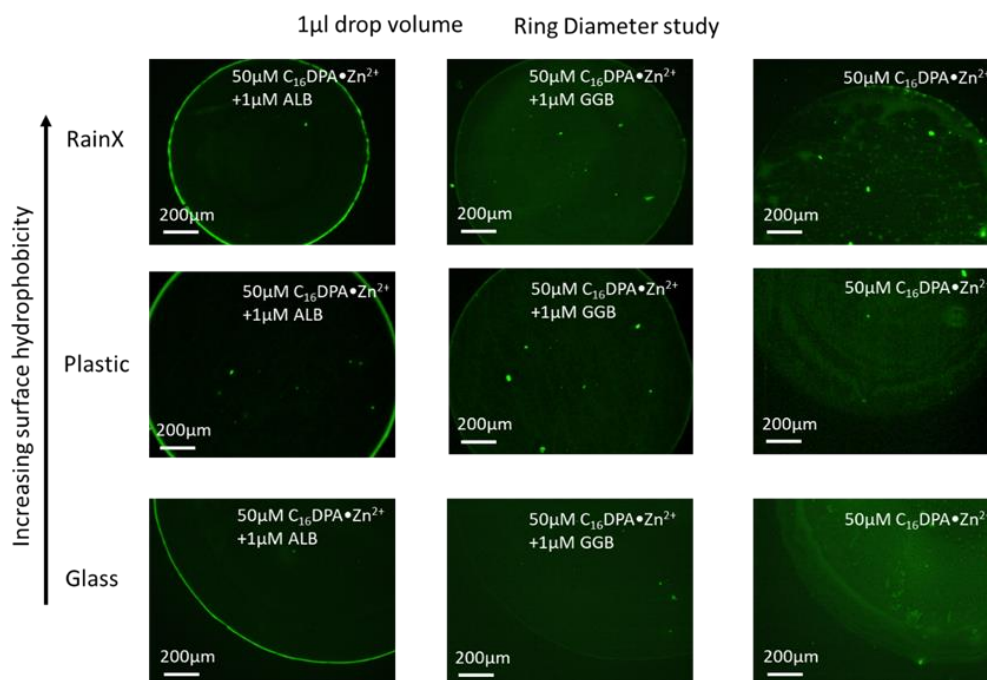


Fig. S25. Coffee ring images of only C₁₆DPA•Zn²⁺, C₁₆DPA•Zn²⁺-ALB and C₁₆DPA•Zn²⁺-GGB complex on glass, plastic and RainX coated glass surface, showing with increasing surface hydrophobicity, ring diameter decreases.

Ring width study

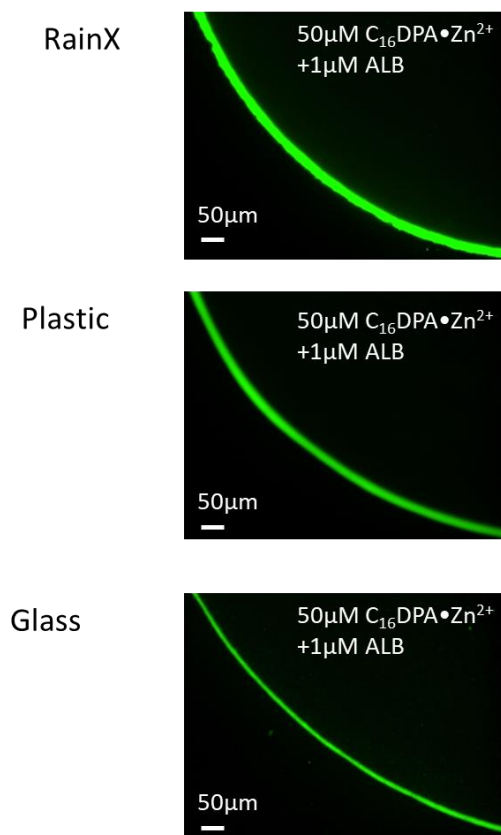


Fig. S26. Coffee ring images of only C₁₆DPA•Zn²⁺, C₁₆DPA•Zn²⁺-ALB and C₁₆DPA•Zn²⁺-GGB complex on glass, plastic and RainX coated glass surface, showing with increasing surface hydrophobicity, ring intensity increases.

Coffee ring formation is an enthalpy-dominated process rather than entropy.⁵⁶ Overall, outward energy flux is main responsible factor for ring-like deposition which increases with increasing contact angle. From both Fig. S25 and S26, we observed shorter and more dense ring formation in surface with higher hydrophobicity.

7.5. Ring formation study at different pH, salt and temperature:

At different pH:

At pH = 6, MES buffer (5 mM)

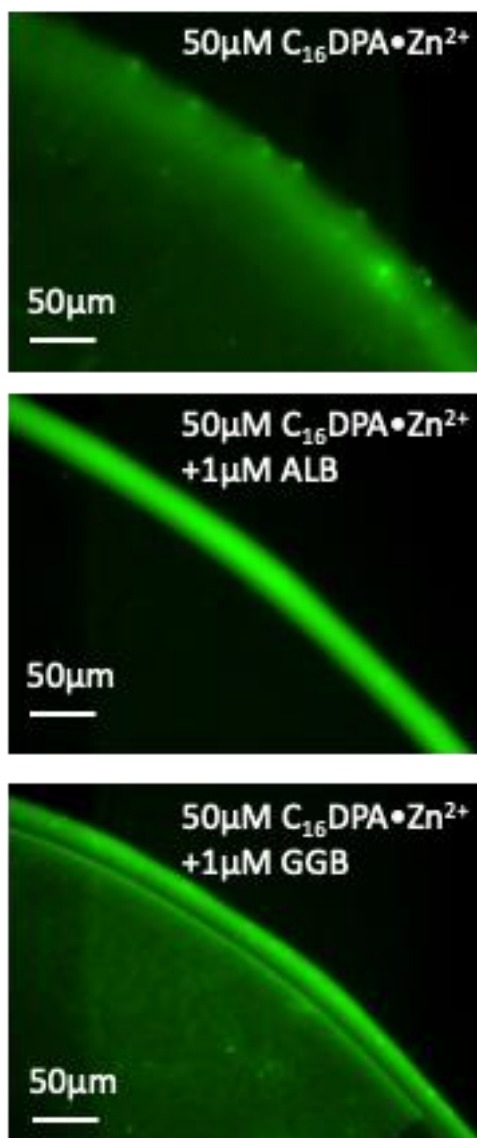


Fig. S27. Fluorescence microscopic images of the spatiotemporal pattern of the ring-like structure formation after the evaporation of a droplet consisting of C₁₆DPA•Zn²⁺, mixed with probe C153 (2 μM) and ALB and GGB in pH = 7 buffer. Experimental conditions: [ALB] = [GGB] = 1 μM, [C153] = 2 μM, [C₁₆DPA•Zn²⁺] = 50 μM, [MES] = 5 mM, pH 6.0, T = 25 °C.

At pH = 8, HEPES buffer (5 mM)

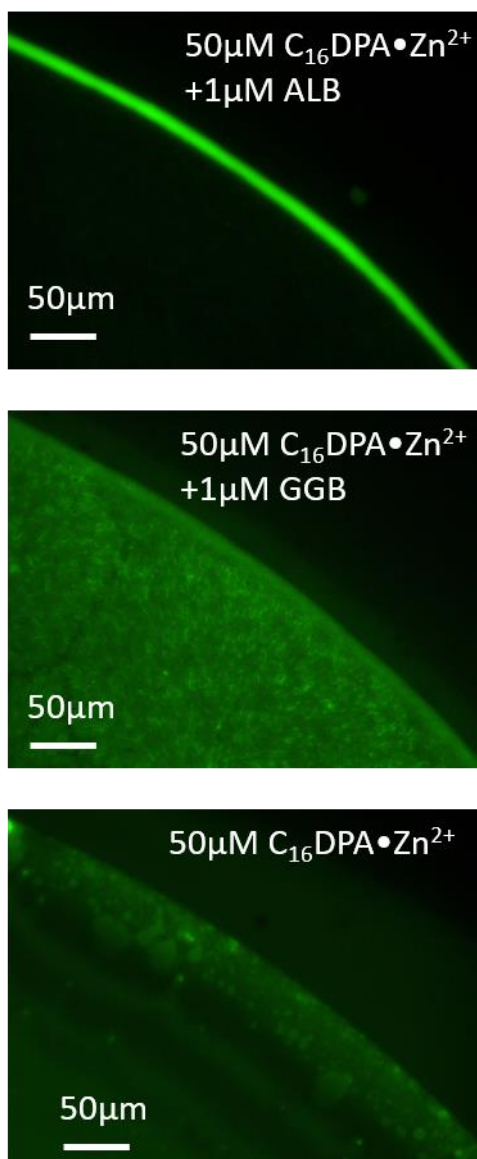


Fig. S28. Fluorescence microscopic images of the spatiotemporal pattern of the ring-like structure formation after the evaporation of a droplet consisting of C₁₆DPA•Zn²⁺, mixed with probe C153 (2 µM) and ALB and GGB in pH = 8 buffer. Experimental conditions: [ALB] = [GGB] = 1 µM, [C153] = 2 µM, [C₁₆DPA•Zn²⁺] = 50 µM, [HEPES] = 5 mM, pH 8.0, T = 25 °C.

At pH = 9, carbonate buffer (5 mM)

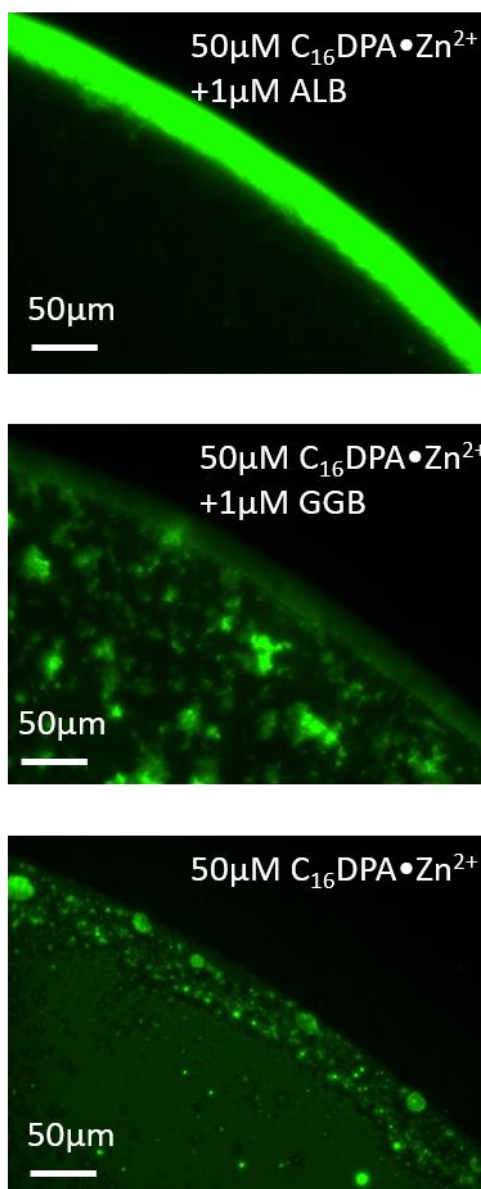


Fig. S29. Fluorescence microscopic images of the spatiotemporal pattern of the ring-like structure formation after the evaporation of a droplet consisting of C₁₆DPA•Zn²⁺, mixed with probe C153 (2 µM) and ALB and GGB in pH = 9 buffer. Experimental conditions: [ALB] = [GGB] = 1 µM, [C153] = 2 µM, [C₁₆DPA•Zn²⁺] = 50 µM, [carbonate] = 5 mM, pH 9.0, T = 25 °C.

Overall, CRE was observed for C₁₆DPA.Zn²⁺-ALB complex and CRS for C₁₆DPA.Zn²⁺-GGB complex across pH range 6 to 9.

In presence of salt

With NaCl (1 mM)

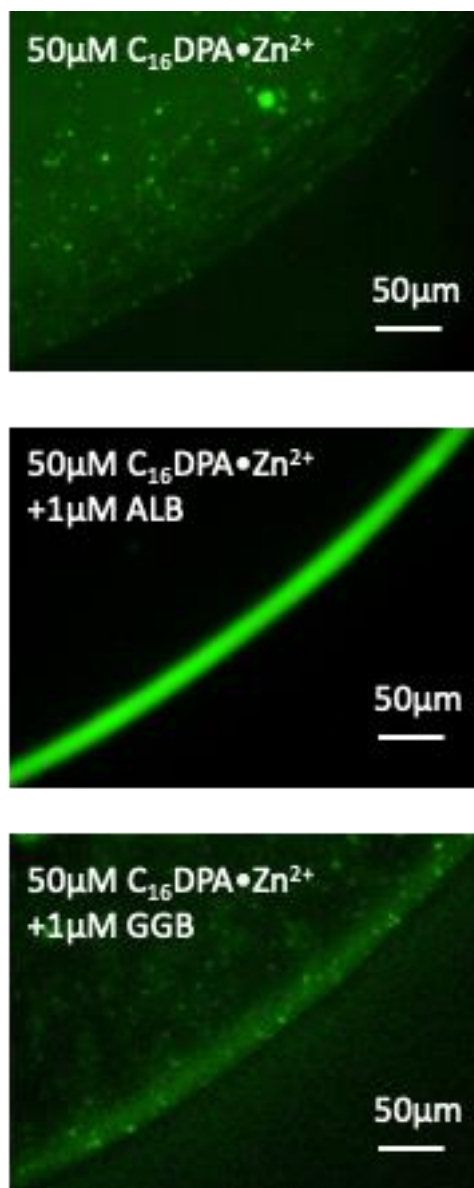


Fig. S30. Fluorescence microscopic images of the spatiotemporal pattern of the ring-like structure formation after the evaporation of a droplet consisting of C₁₆DPA•Zn²⁺, mixed with probe C153 (2 μM) and ALB and GGB in presence of NaCl (1 mM). Experimental conditions: [ALB] = [GGB] = 1 μM, [C153] = 2 μM, [C₁₆DPA•Zn²⁺] = 50 μM, T = 25 °C.

With Na_3PO_4 (1 mM)

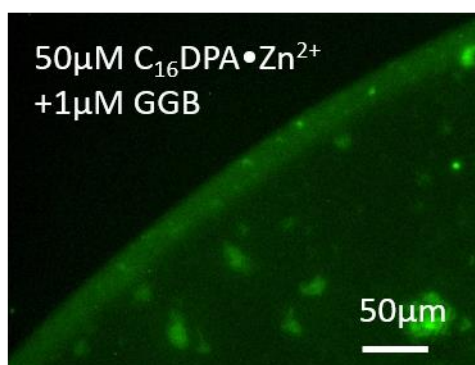
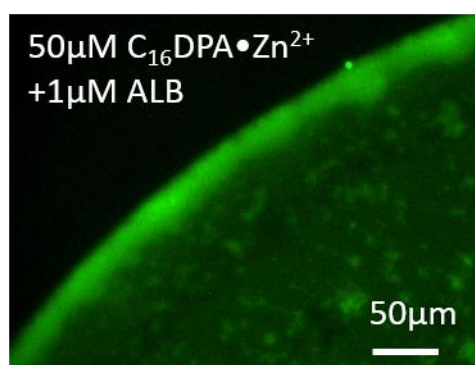
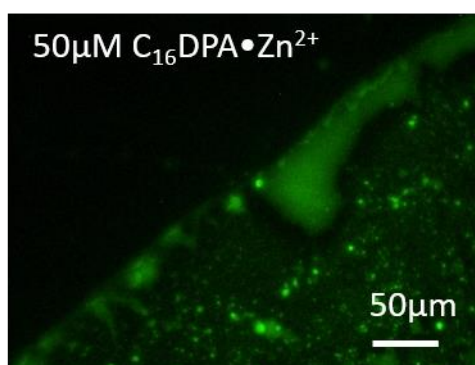


Fig. S31. Fluorescence microscopic images of the spatiotemporal pattern of the ring-like structure formation after the evaporation of a droplet consisting of $\text{C}_{16}\text{DPA}\cdot\text{Zn}^{2+}$, mixed with probe C153 (2 μM) and ALB and GGB in presence of Na_3PO_4 (1 mM). Experimental conditions: $[\text{ALB}] = [\text{GGB}] = 1 \mu\text{M}$, $[\text{C153}] = 2 \mu\text{M}$, $[\text{C}_{16}\text{DPA}\cdot\text{Zn}^{2+}] = 50 \mu\text{M}$, $T = 25 \text{ }^\circ\text{C}$.

In case of NaCl, CRE was clearly observed for $\text{C}_{16}\text{DPA}\cdot\text{Zn}^{2+}$ -ALB complex but not so prominent in case of Na_3PO_4 . Actually, phosphate ion has very high binding affinity with the Zn^{2+} -containing surfactant headgroup, resulting formation of larger structures.⁵³ Therefore, the formation of solely ALB-driven surfactant complex gets hindered as observed from the above images (Fig. S31).

With temperature

At 55°C

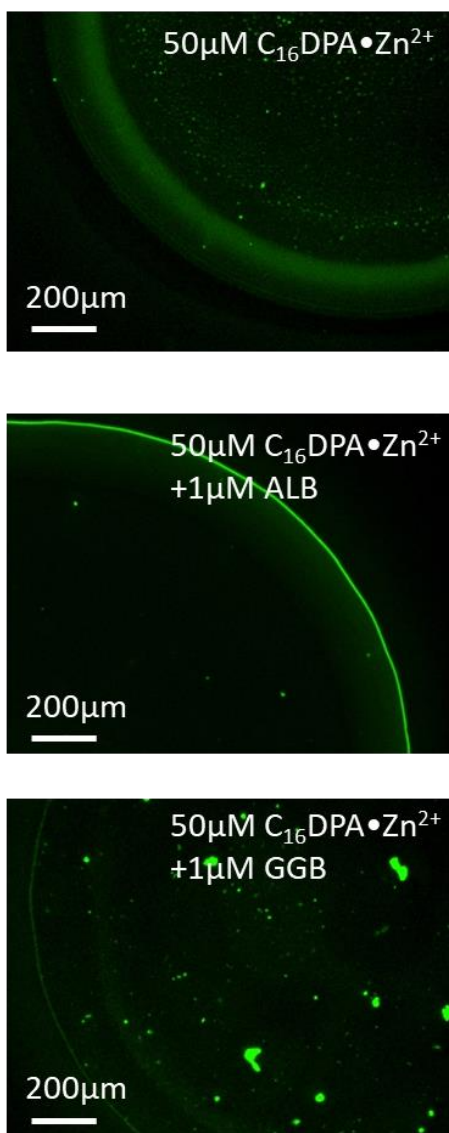


Fig. S32. Fluorescence microscopic images of the spatiotemporal pattern of the ring-like structure formation after the evaporation of a droplet consisting of C₁₆DPA•Zn²⁺, mixed with probe C153 (2 µM) and ALB and ALB. Experimental conditions: [ALB] = [GGB] = 1 µM, [C153] = 2 µM, [C₁₆DPA•Zn²⁺] = 50 µM, T = 55 °C. At higher temperature due to much faster evaporation, thickening of ring for Fluorescence microscopic images of the spatiotemporal pattern of the ring-like structure formation after the evaporation of a droplet consisting of C₁₆DPA•Zn²⁺, mixed with probe C153 (2 µM) and ALB and GGB. Experimental conditions: [ALB] = [GGB] = 1 µM, [C153] = 2 µM, [C₁₆DPA•Zn²⁺] = 50 µM, T = 55 °C. At higher temperature due to much faster evaporation, chance of observation of coffee ring is high.^{S7} For this, even in case of GGB, CRE was faintly observed.

8. DLS Measurement with time:

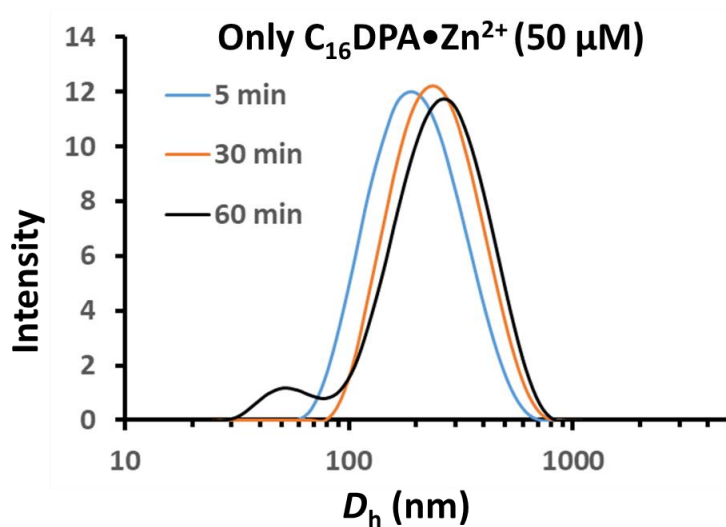


Fig. S33: Hydrodynamic diameter of the assemblies measured at different time intervals via dynamic light scattering (DLS). Experimental conditions: $[C_{16}DPA \bullet Zn^{2+}] = 50 \mu M$, $[HEPES] = 5 \text{ mM}$, $\text{pH } 7.0$, $T = 25 \text{ }^\circ\text{C}$. The measurements were taken upto 60 minutes.

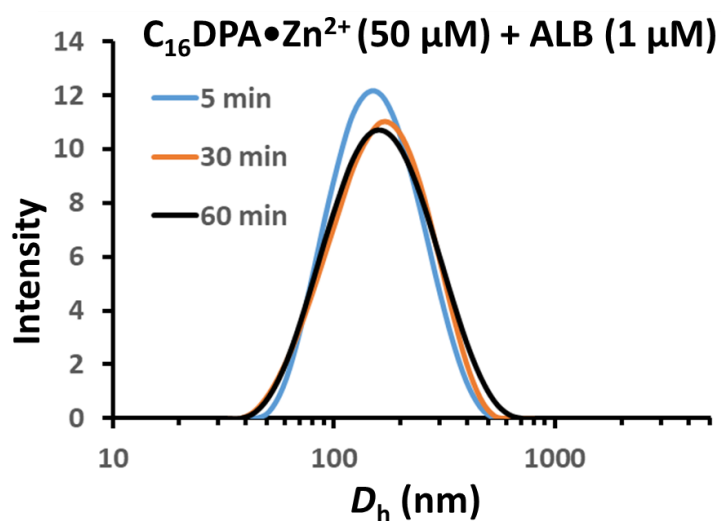


Fig. S34: Hydrodynamic diameter of the Surfactant-ALB conjugates measured at different time intervals via dynamic light scattering (DLS). Experimental conditions: $[C_{16}DPA \bullet Zn^{2+}] = 50 \mu M$, $[ALB] = 1 \mu M$, $[HEPES] = 5 \text{ mM}$, $\text{pH } 7.0$, $T = 25 \text{ }^\circ\text{C}$. The measurements were taken upto 60 minutes.

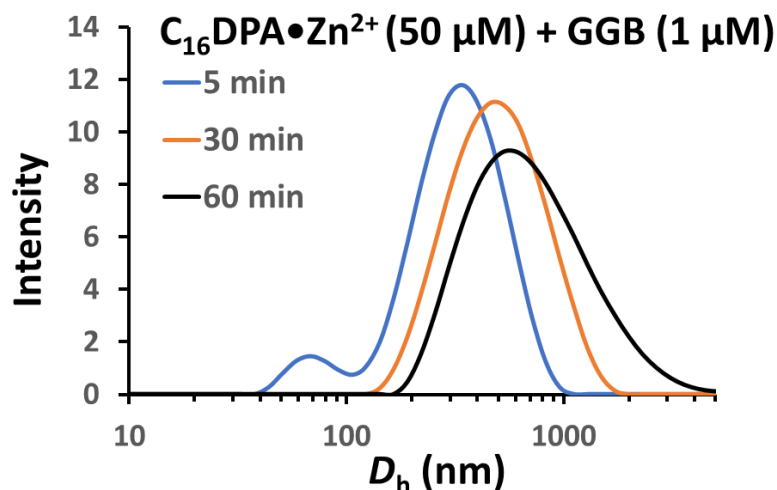


Fig. S35: Hydrodynamic diameter of the Surfactant-GGB conjugates measured at different time interval via dynamic light scattering (DLS). Experimental conditions: $[C_{16}DPA \bullet Zn^{2+}] = 50 \mu M$, $[GGB] = 1 \mu M$, $[HEPES] = 5 \text{ mM}$, pH 7.0, $T = 25 \text{ }^\circ\text{C}$. The measurements were taken upto 60 minutes.

9. Anisotropy Measurements:

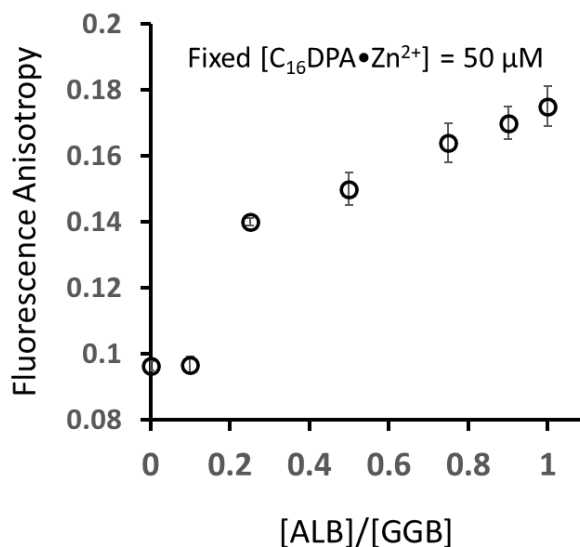


Fig. S36: Anisotropy values of the system containing different concentration of proteins (ALB and GGB) with Zn(II)-metallo-surfactant. Experimental conditions: $[ALB] \text{ \& } [GGB] = 1 \mu M$, $[C153] = 2 \mu M$, $[C_{16}DPA \bullet Zn^{2+}] = 50 \mu M$, $[HEPES] = 5 \text{ mM}$, pH 7.0, $T = 25 \text{ }^\circ\text{C}$.

We have checked the fluorescence anisotropy of the hydrophobic probe C153 in presence of surfactant protein conjugates. It is to be noted here that fluorescence anisotropy is a measure of rotational mobility of the enzyme which increase in a confined environment.^[S5] Anisotropy data clearly suggest that restricted mobility of C153 takes place when the concentration of ALB was high. Overall, fluorescent anisotropic values also followed similar trend of coffee ring width.

10. Coffee Ring Pattern with FITC tagged Proteins:

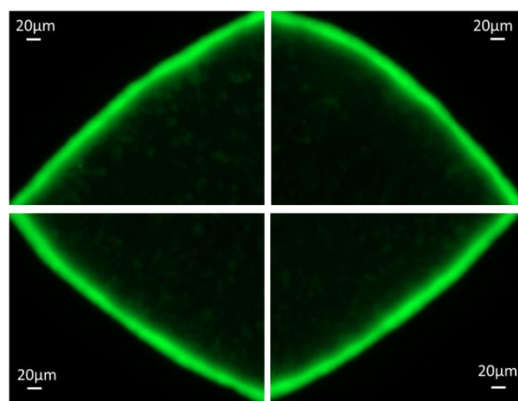


Fig. S37. Fluorescence microscopic images of the spatiotemporal pattern of the ring-like structure formation after the evaporation of a droplet consisting of $C_{16}DPA \bullet Zn^{2+}$, mixed with 1 μM FITC-tagged ALB. Experimental conditions: [FITC-ALB] = 1 μM , $[C_{16}DPA \bullet Zn^{2+}] = 50 \mu M$, [HEPES] = 5 mM, pH 7.0, T = 25 $^{\circ}C$.

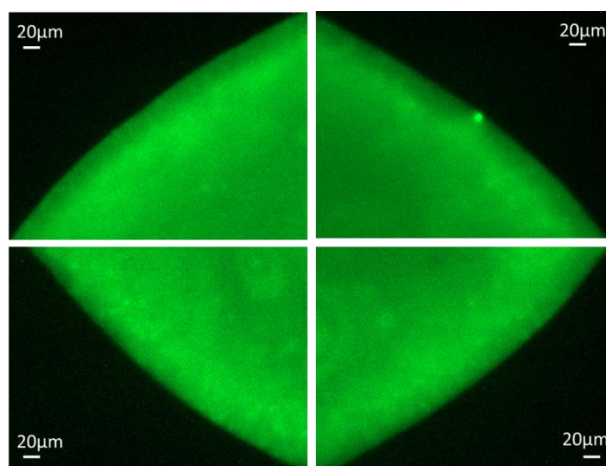


Fig. S38. Fluorescence microscopic images of the spatiotemporal pattern of the ring-like structure formation after the evaporation of a droplet consisting of $C_{16}DPA \bullet Zn^{2+}$, mixed with 0.5 μM FITC-tagged GGB. Experimental conditions: [FITC-GGB] = 0.5 μM , $[C_{16}DPA \bullet Zn^{2+}] = 50 \mu M$, [HEPES] = 5 mM, pH 7.0, T = 25 $^{\circ}C$.

Upon performing coffee ring experiment with fluorescently labelled (tagged with fluorescein isothiocyanate (FITC))-ALB and GGB-conjugated with $C_{16}DPA \bullet Zn^{2+}$ without using external probe, C153, we also observed clear coffee ring formation with (FITC-ALB)- $C_{16}DPA \bullet Zn^{2+}$ conjugate and coffee disk formation with (FITC-GGB) conjugate confirming the presence of protein in ring or disk along with the assembly, similar to our observation in SEM and AFM (Fig. S37-S38 and Fig. S18 + S20 +S21).

11. Coffee Ring Patterns with CTAB:

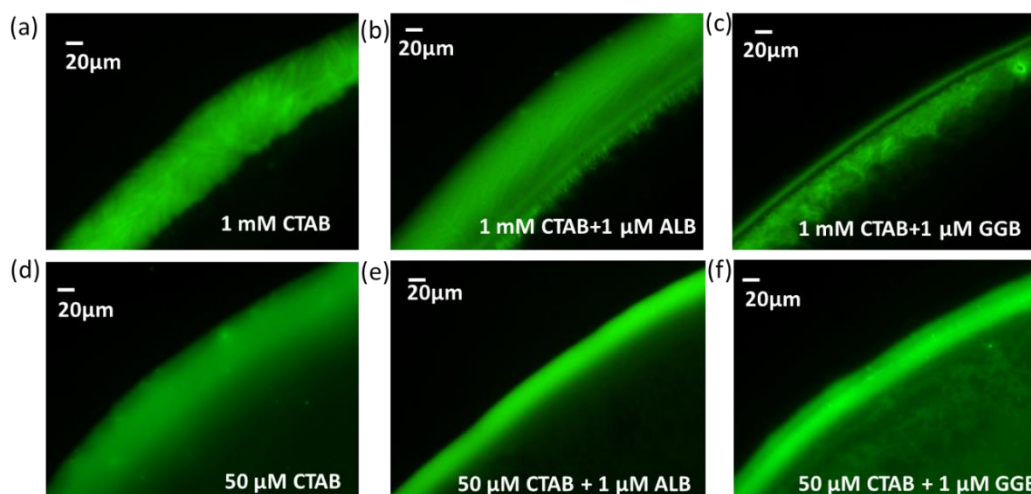


Fig. S39. Fluorescence microscopic images of the spatiotemporal pattern of the ring-like structure formation after the evaporation of a droplet consisting of CTAB, mixed with probe C153 (2 μM) and ALB and GGB in buffer. Experimental conditions: [ALB] & [GGB] = 1 μM, [C153] = 2 μM, [CTAB]= 50 μM & 1 mM, [HEPES] = 5 mM, pH 7.0, T = 25 °C.

12. Coffee Ring Patterns with SDS:

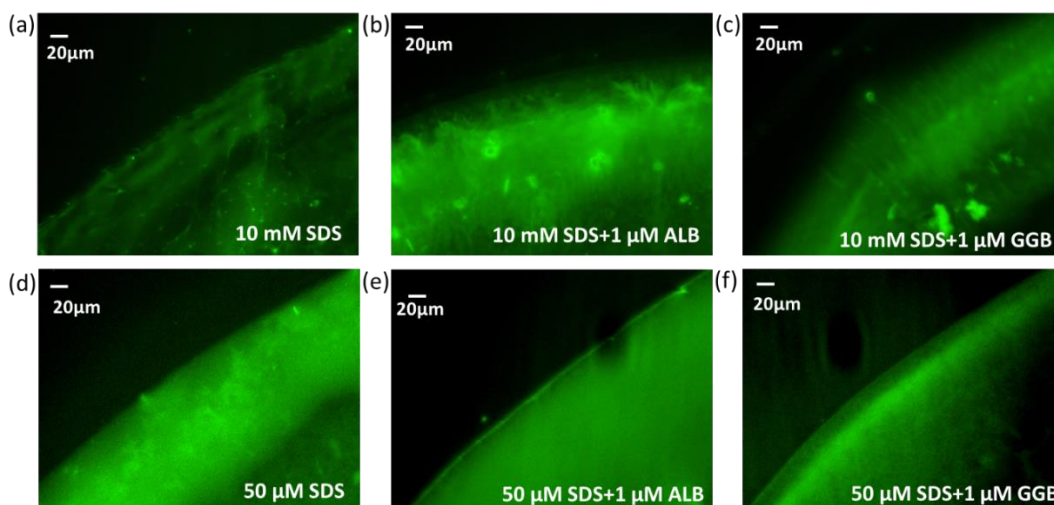
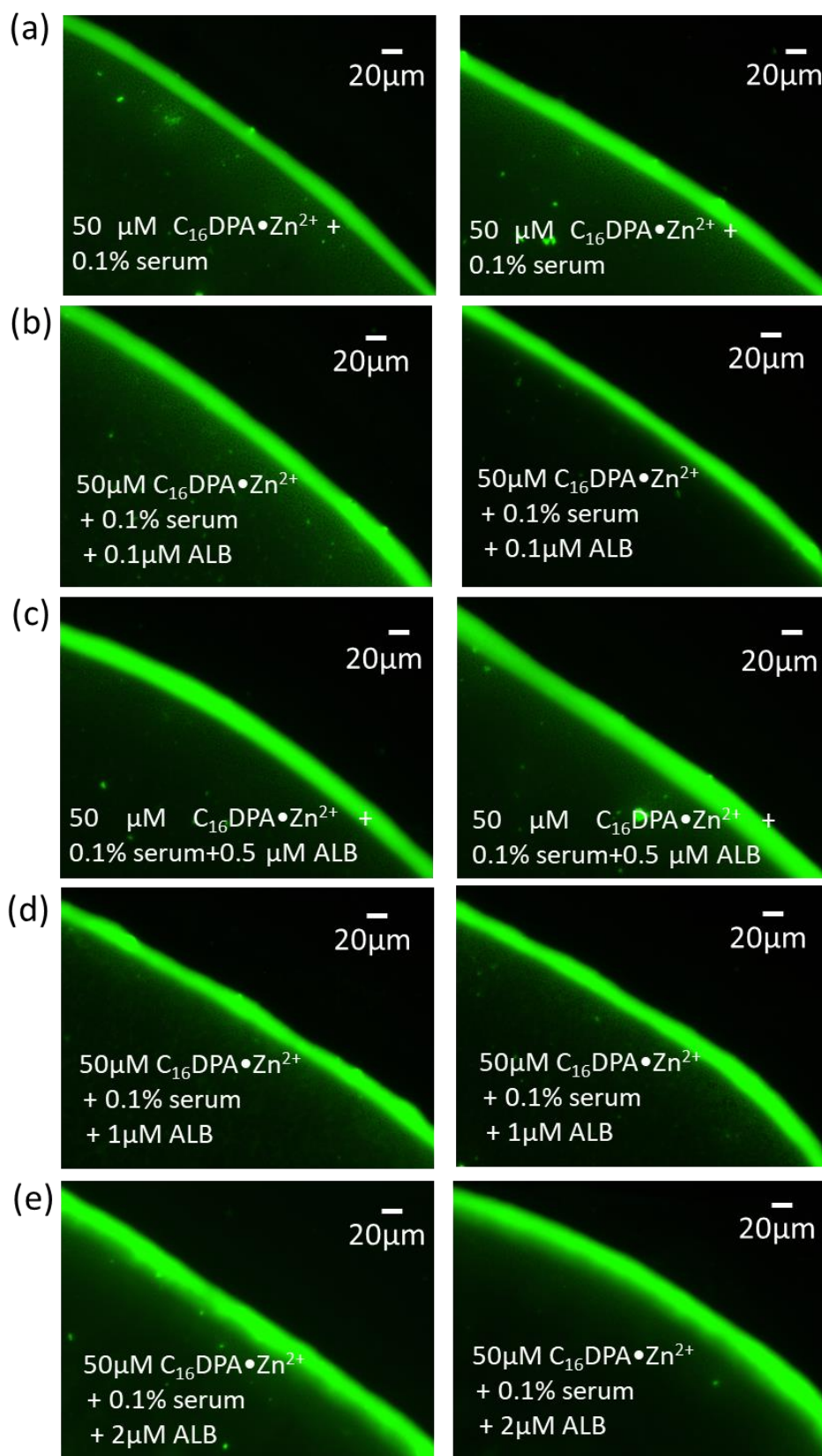


Fig. S40: Fluorescence microscopic images of the spatiotemporal pattern of the ring-like structure formation after the evaporation of a droplet consisting of SDS, mixed with probe C153 (2 μM) and ALB and GGB in buffer. Experimental conditions: [ALB] & [GGB] = 1 μM, [C153] = 2 μM, [SDS]= 50 μM & 10 mM, [HEPES] = 5 mM, pH 7.0, T = 25 °C.

We also checked CRE with CTAB and SDS micelle using C153 probe, with ALB and GGB. However, no distinct differences were obtained in either cases which might be due to their low protein binding affinity (Fig. S39-S40, ESI).

13. Coffee Ring Patterns with Serum:



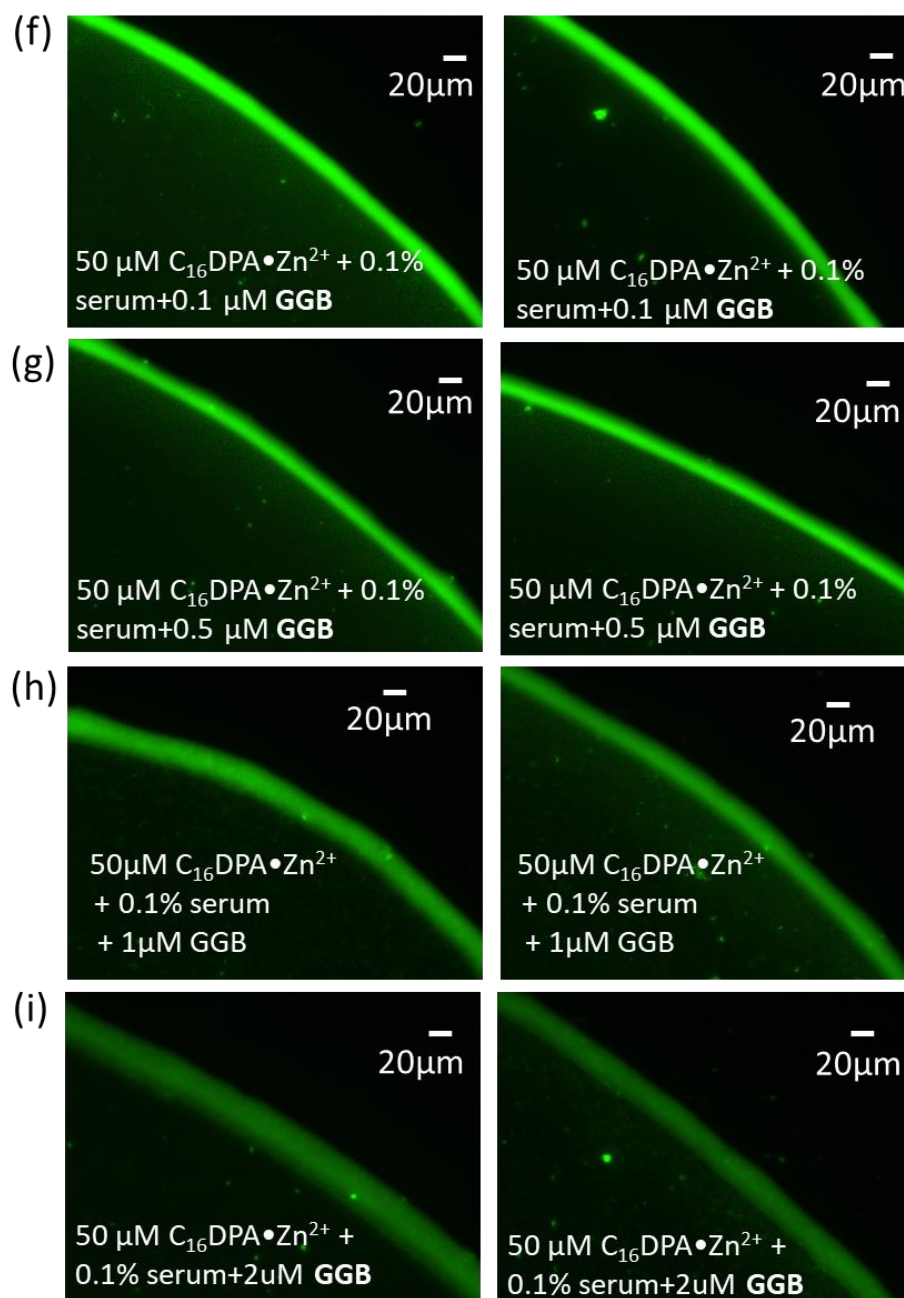


Fig.S41. Fluorescence microscopic images (a)-(i) of the spatiotemporal pattern of the ring-like structure formation after the evaporation of a droplet consisting of blood serum mixed with $C_{16}DPA \cdot Zn^{2+}$, probe C153 (2 μM) and different amount of ALB and GGB in the buffer. Experimental conditions: [ALB] & [GGB] = 0.1-2 μM , [C153]= 2 μM , [$C_{16}DPA \cdot Zn^{2+}$]= 50 μM , [Serum]= 0.1% [HEPES] = 5 mM, pH 7.0, T = 25 $^{\circ}C$.

The normal concentration of albumin and gamma-globulin in human serum lies in the range of $600 \pm 100 \mu M$ and $75 \pm 25 \mu M$, respectively. In our study, 0.1% serum is used, which contains $0.6 \pm 0.1 \mu M$ ALB and $0.075 \pm 0.025 \mu M$ GGB. On spiking the 0.1% serum with 0.5 μM ALB, the concentration of albumin in human serum increases by 2-fold, also on spiking with 0.1 μM GGB, the concentration of gamma-globulin increases by 2-fold.

Spiked ALB concentration in 0.1% serum	Effective increase in ALB concentration in serum*	Percentage increase in ALB concentration in serum
2 μM	2600 μM	75 %
1 μM	1600 μM	60 %
0.5 μM	1100 μM	45 %
0.1 μM	700 μM	15 %

Spiked GGB concentration in 0.1% serum	Effective increase in GGB concentration in serum*	Percentage increase in GGB concentration in serum
2 μM	2075 μM	95 %
1 μM	1075 μM	90 %
0.5 μM	575 μM	85 %
0.1 μM	175 μM	55 %

*Error is in the limit of 10%.

14. References:

- [S1] F. Kilár, I. Simon, S. Lakatos, F. Vonderviszt, G. A. Medgyesi and P. Závodszy, *Eur. J. Biochem.*, 1985, **147**, 17–25.
- [S2] W. B. Bridgman, *J. Am. Chem. Soc.*, 1946, **68**, 857–861.
- [S3] Priyanka, S. Kaur Brar and S. Maiti, *ChemNanoMat*, 2022, **8**, e202100498.
- [S4] S. Rani, B. Dasgupta, G. K. Bhati, K. Tomar, S. Rakshit and S. Maiti, *ChemBioChem*, 2021, **22**, 1285–1291.
- [S5] D. Jameson and J. Ross, *Chem. Rev.*, 2010, **110**, 2685 —2708 .
- [S6] S. Choi and G. Birada, *J. Phys. Chem. B* 2017, **121**, 7359-7365.
- [S7] R. Sliz, J. Czajkowski and T. Fabritius, *Langmuir* 2020, **36**, 9562-9570.